

Meso-Scale Predictions of Microstructure Following Laser-Interaction via kMC Simulation

J. Madison, V. Tikare

¹Sandia National Laboratories, Albuquerque NM

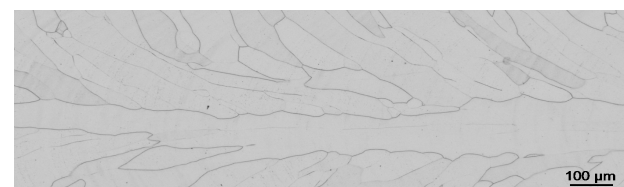
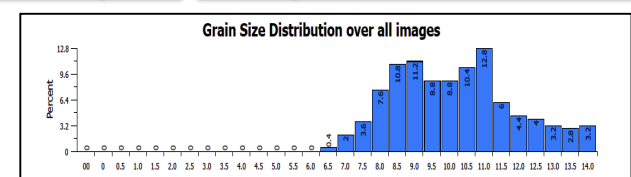
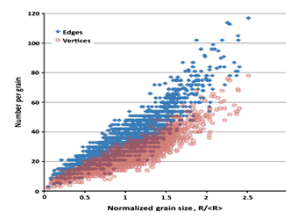
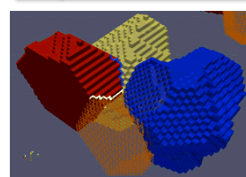
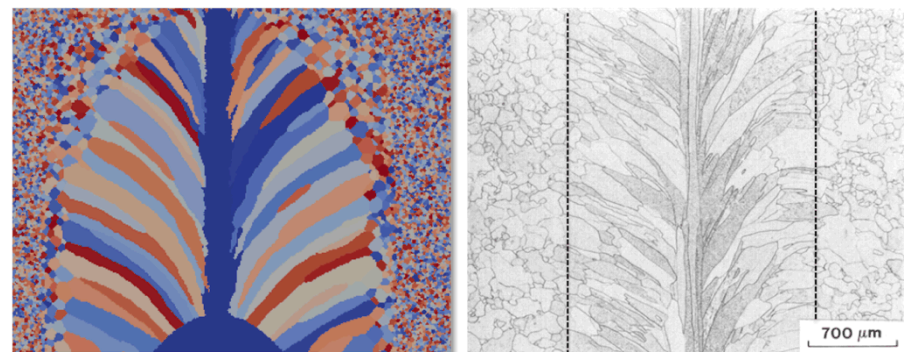


3rd World Congress on Integrated
Computational Materials Engineering
May 31 - June 4, 2015 • Colorado Springs, Colorado, USA



Sandia National Laboratories is a multi-program laboratory managed and operated by Sandia Corporation, a wholly owned subsidiary of Lockheed Martin Corporation, for the U.S. Department of Energy's National Nuclear Security Administration under contract DE-AC04-94AL85000. SAND No. 2015-XXXX

*Exceptional service
in the national interest*



Outline

- Background
- Simulation Framework
- Equations of State
- Kinetics of Evolution
- Applicability to Welds
- Results
 - Experimental Results
 - Simulation Results
 - Experimental/Simulation Validation
- Future Work
- Summary

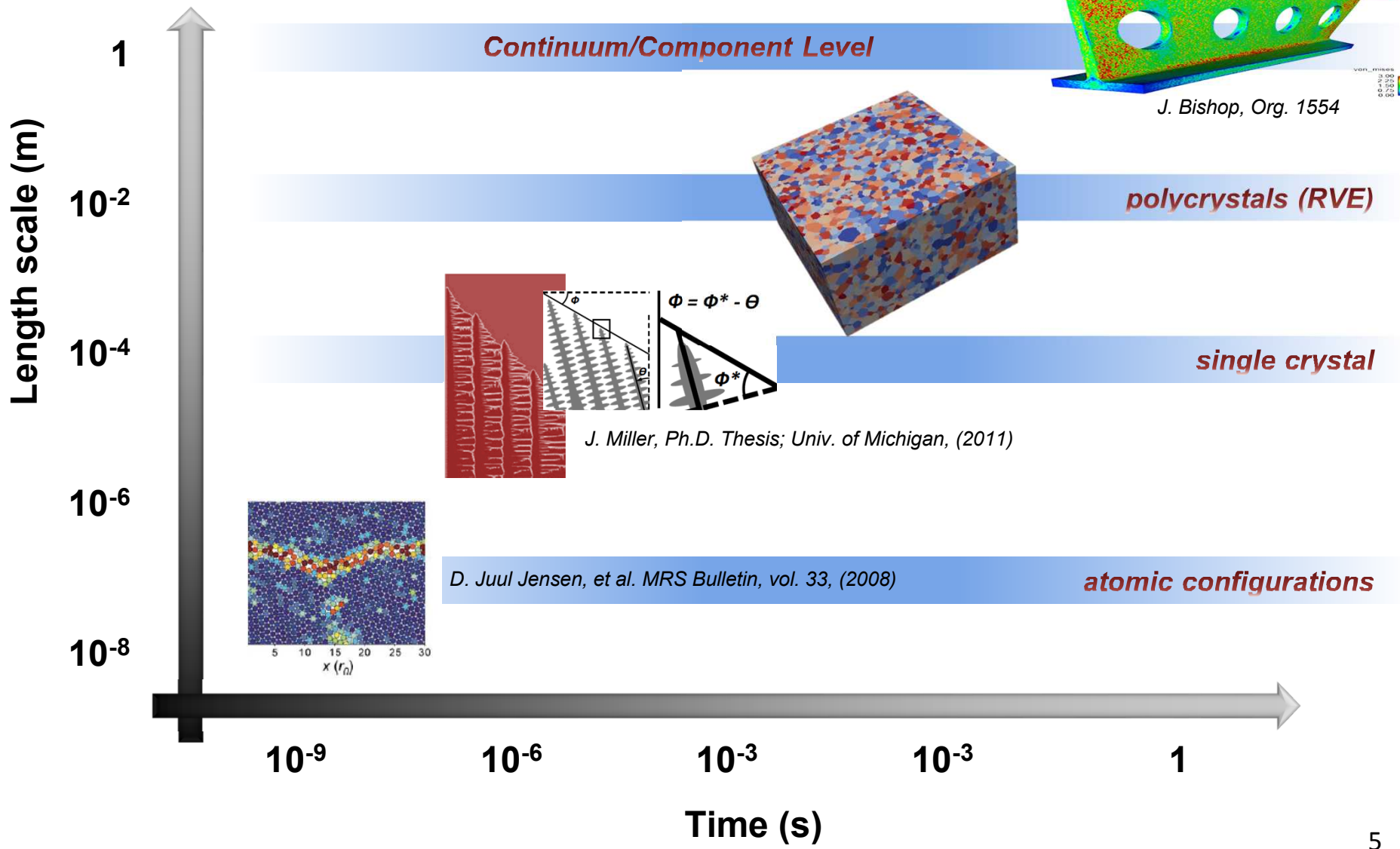
Background I

- **Metallurgists & ceramists have long agreed that most “homogenous” materials possess several levels of structure between the atomic and the macroscopic**
 - Dislocation networks
 - Precipitate dispersions
 - Grains & grain boundaries
 - Phases & phase boundaries
- **Microstructure influences, governs, dictates and/or explains**
 - Mechanical properties
 - Thermal properties
 - Electrical properties
 - Temporal behavior
- **Microstructural evolution has been a focus of study for over a century**
 - J.E. Burke & D. Turnbull, *Prog. Metal Phys.*, 3 (1952) p. 220

Background II

- Computational simulations of microstructural evolution can be traced back to the 1950's
 - R.L. Fullman, *Metal Interfaces* (Cleveland, OH: ASM, 1952), p. 179
 - manual calculations of grain growth
- Many computational tools have been developed with a focus on microstructural evolution
 - **Thermo-Calc** – thermodynamic predictions
 - **PanDat** – thermodynamic predictions
 - **ProCast** – solidification
 - **JMatPro** –
 - **Micress** –
 - **Dante** –
 - **LAMMPS** – molecular dynamic simulation
 - **VaSP** – density functional theory
 - **PrecipiCalc** –

Background III

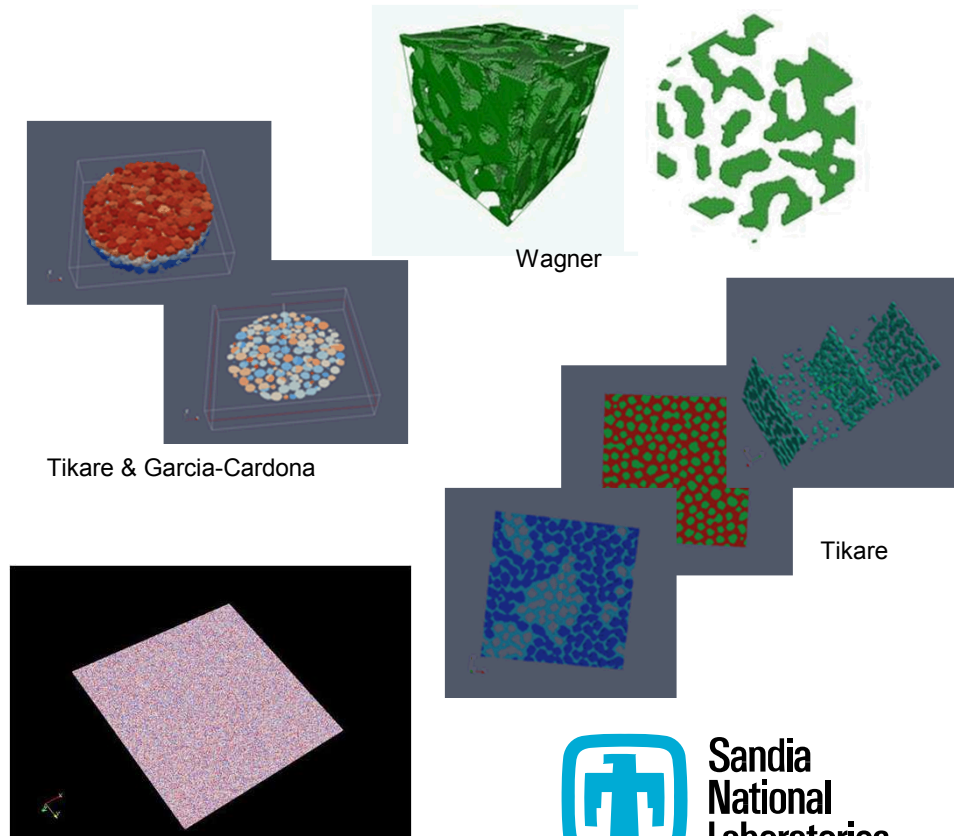


Simulation Framework

SPPARKS

Kinetic Monte Carlo via Stochastic Parallel PARticle Kinetic Simulator

- Development a new user application for SNL's SPPARKS open-source environment
- Treat grain growth + dynamic recrystallization events simultaneously
- Incorporate probabilistic cellular-automaton approach to more accurately capture realistic kinetics (KJMA rates)
- Toward prediction of microstructural evolution in irradiated materials beyond currently established NRC regulations



<http://spparks.sandia.gov>

Thermodynamic Equations of State

- Complex EOS can be constructed with two basic energy components :
 - A volumetric free energy term, E_{vol}
 - An interfacial free energy term, E_{int}
 - These basic components are the basis for grain growth, recrystallization, sintering, abnormal grain growth, etc.

$$E = E_{vol} + E_{int}$$

$$E = \sum_{i=1}^N \left(E_{vol}(q_i) + \frac{1}{2} \sum_{j=1}^n J(1 - \delta_{ij}) \right)$$

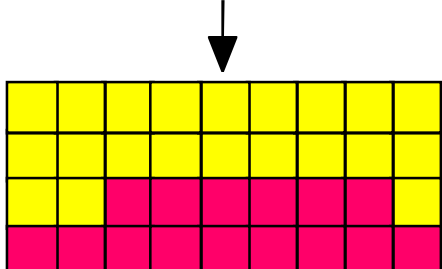
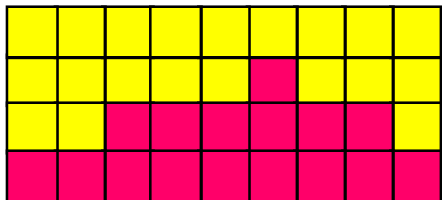
where;
 N = # of sites
 n = # of neighbors
 j = neighboring sites

Kinetics of Evolution I

- Domain ensemble is statistically evolved to mimic atomistic diffusive processes.
- Boltzmann statistics are used to govern the evolutionary process

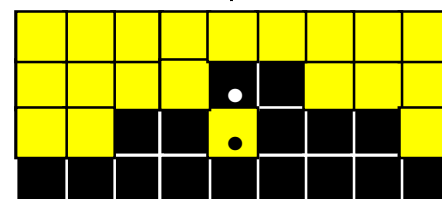
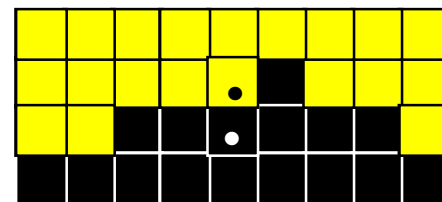
$$P = \begin{cases} 1 & \text{for } E \leq 0 \\ \exp\left(\frac{-\Delta E}{kT}\right) & \text{for } E > 0 \end{cases}$$

**curvature driven
grain growth**



voxel membership change

**diffusive particle
migration**



voxel membership change

Ensemble evolution

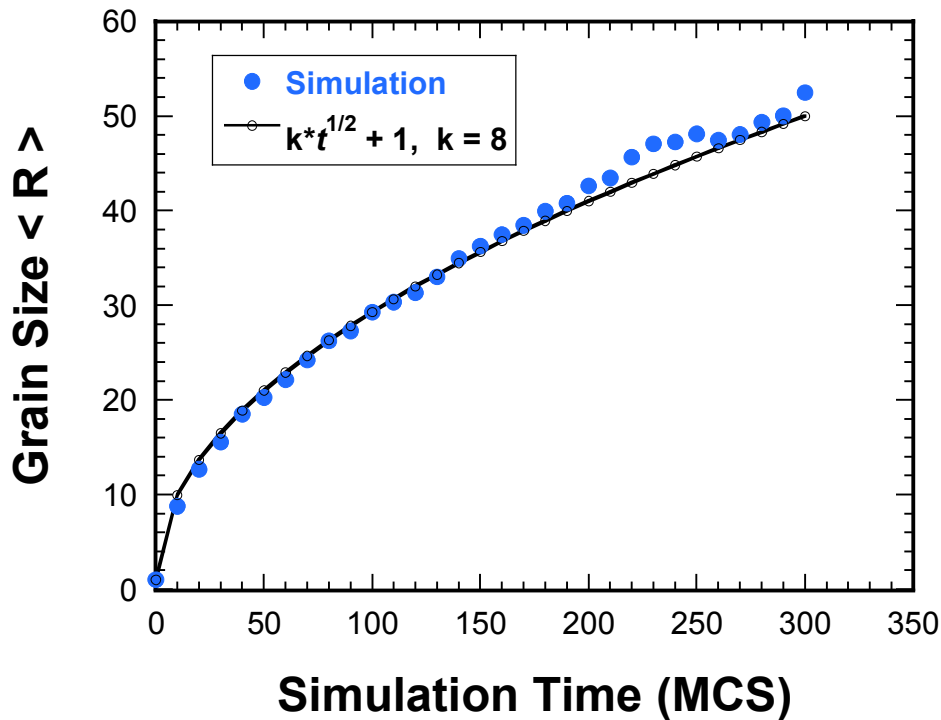
Minimization of Total
Free Energy

Kinetics of
Microstructural
Evolution



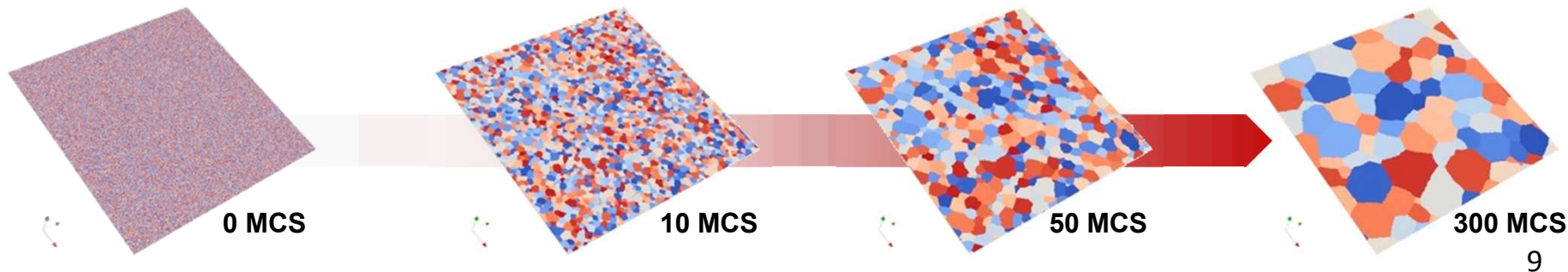
Kinetics of Evolution II

Traditional Grain Growth



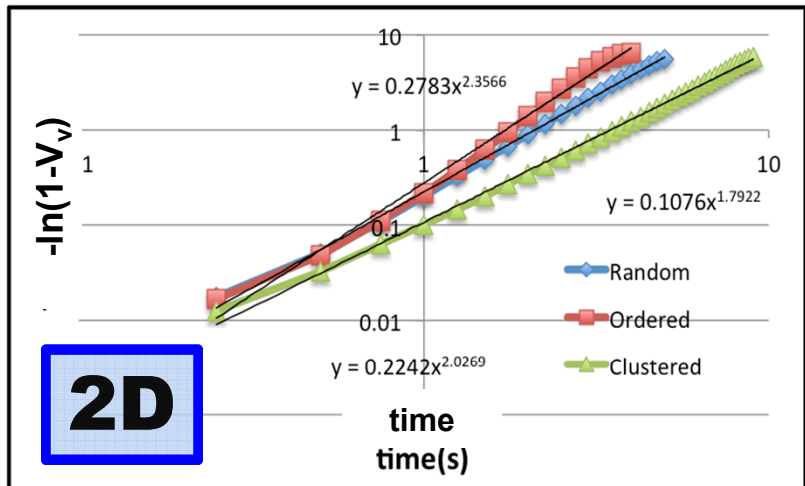
$$E_{GG} = \frac{1}{2} \sum_{i=1}^N \sum_{j=1}^{neigh} [1 - \delta(q_i, q_j)]$$

$$P = \begin{cases} \exp\left(\frac{-\Delta E}{k_B T_S}\right) & \text{if } \Delta E > 0 \\ 1 & \text{if } \Delta E \leq 0 \end{cases}$$



Kinetics of Evolution III

Recrystallization, KJMA Exponents



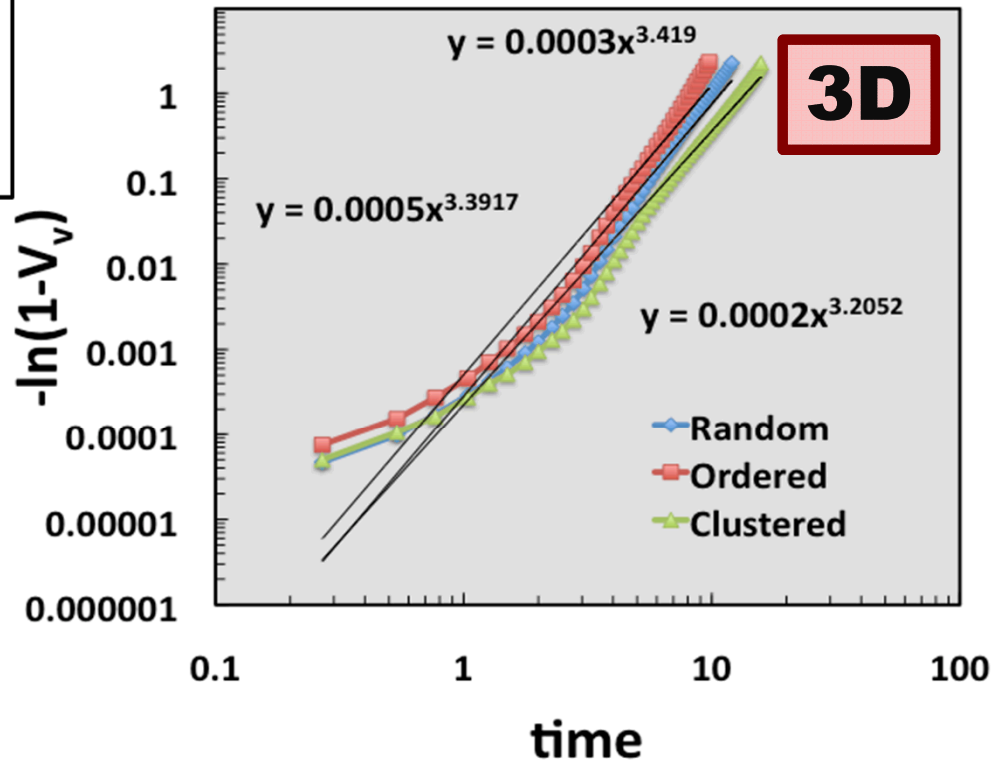
For site saturated nuclei

1D growth : $n \sim 1$

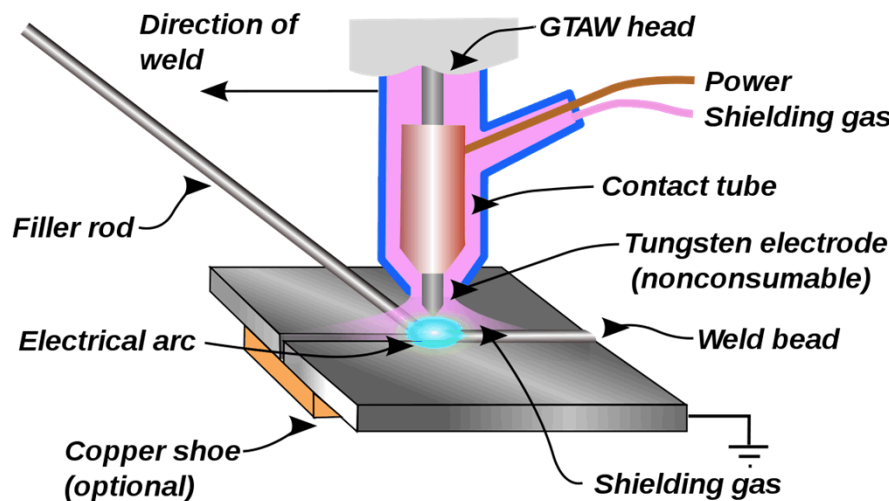
2D growth : $n \sim 2$

3D growth : $n \sim 3$

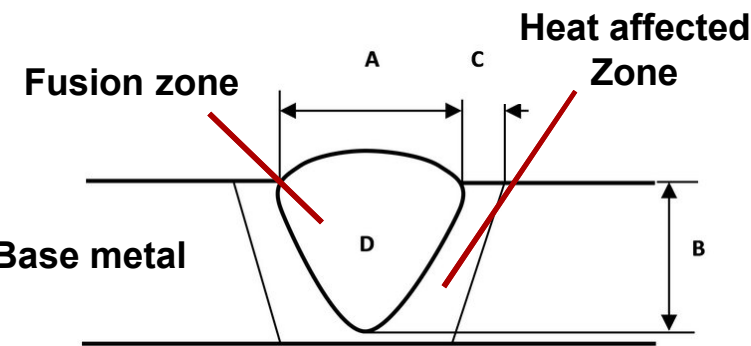
$$\log(-\ln(1 - V_v)) = n \log(t)$$



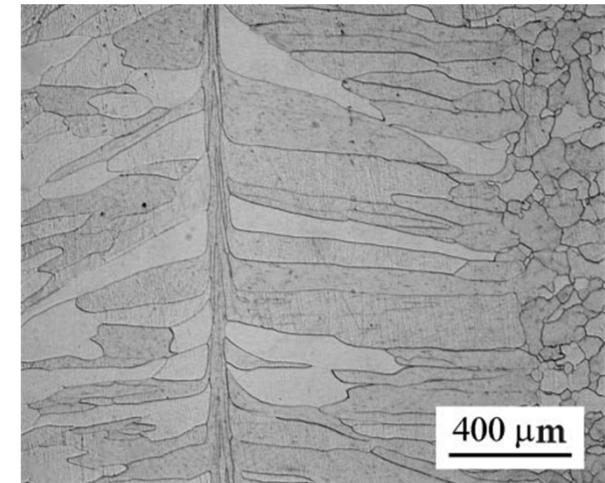
Applicability to Welds



Gas Tungsten Arc Welding



C. Neelamegam et al. *J. Int. Learning Sys. & Apps*, vol. 5 (2013), pp. 39-47



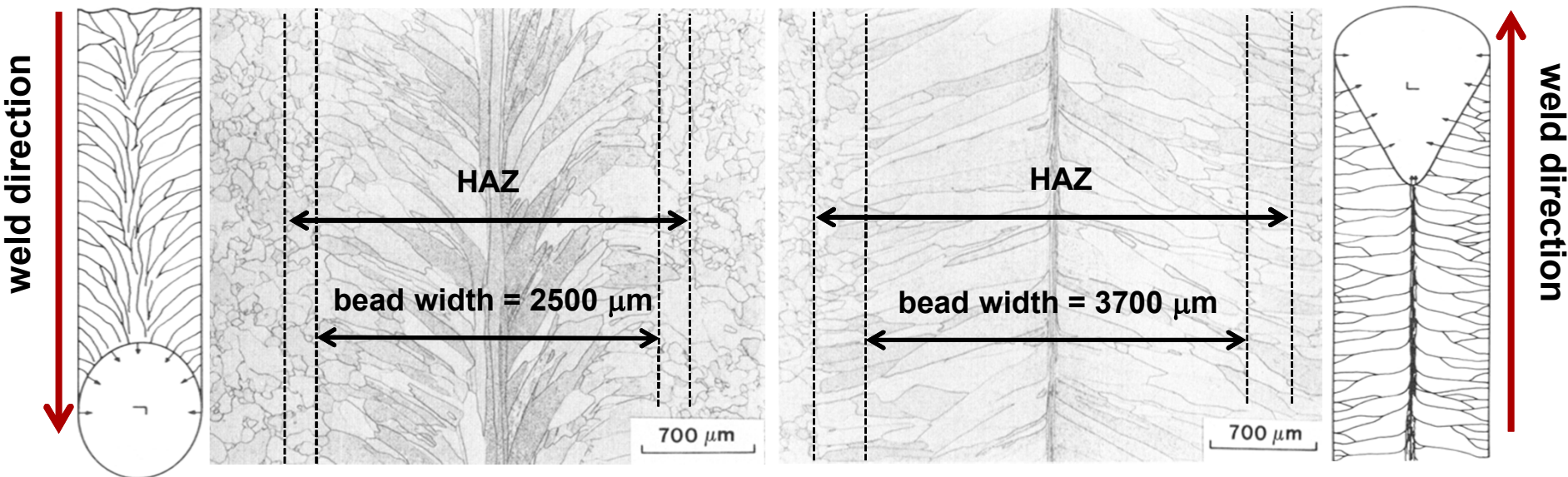
McKamey et al., *Sci & Tech. of Welding & Joining*, vol. 5 (2000), pp. 297-303

Experimental Microstructures

Welding of Iridium, DOP-26

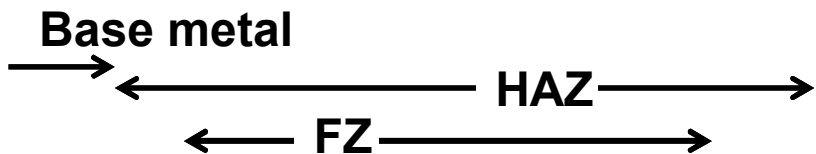
Microstructure is primarily a function of :

- bead width: 3.7, 2.5 mm
- Heat input: determined bead width
- Weld speed: 76 cm/min

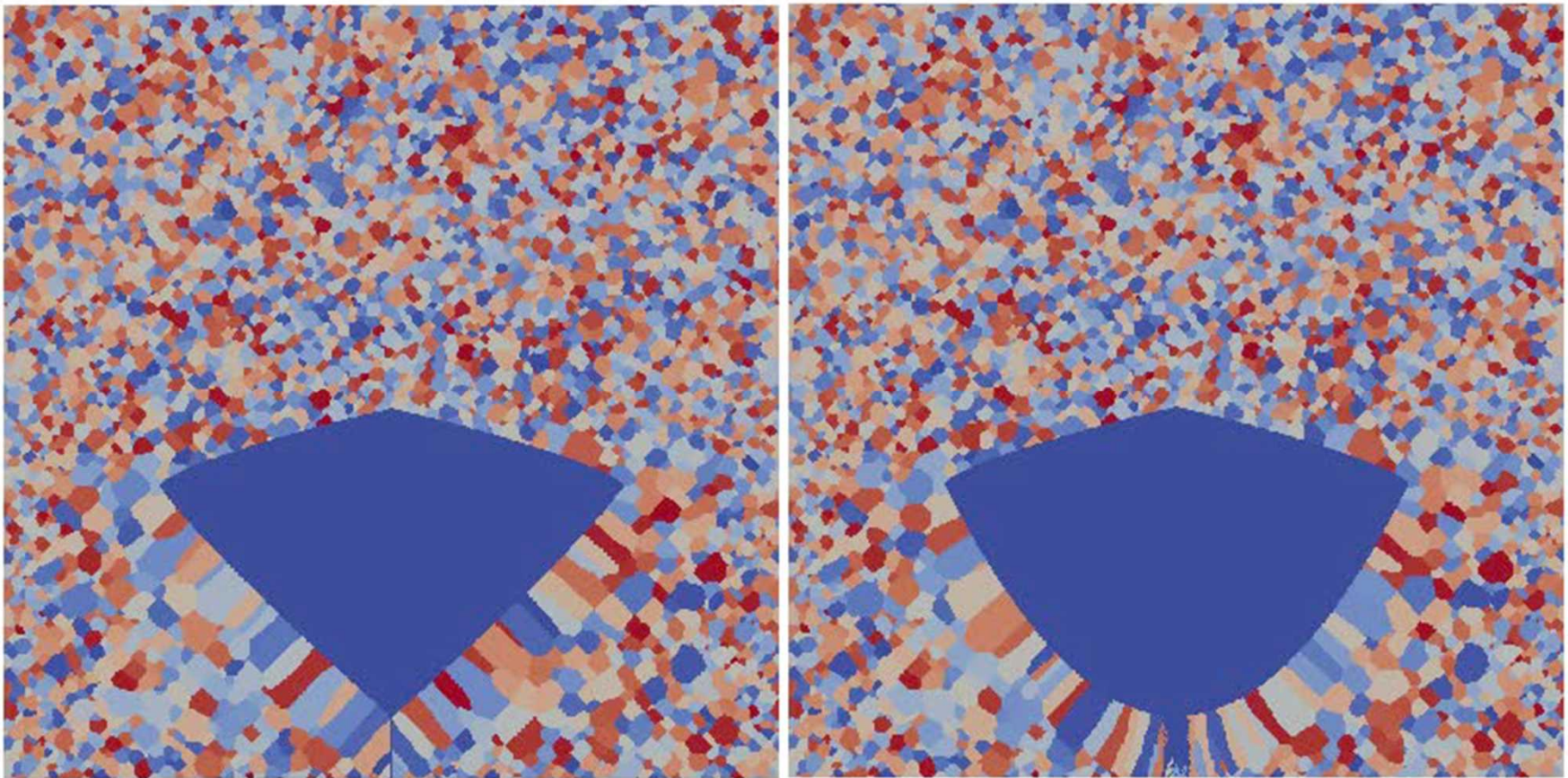


C. Liu & S. David, *Weld Metal Grain Structure and Mechanical Properties of a Th-Doped Ir-0.3 Pct W Alloy* **Met Trans A**. vol. 13 A, (1982) pp. 1043-1053

Simulated Microstructures



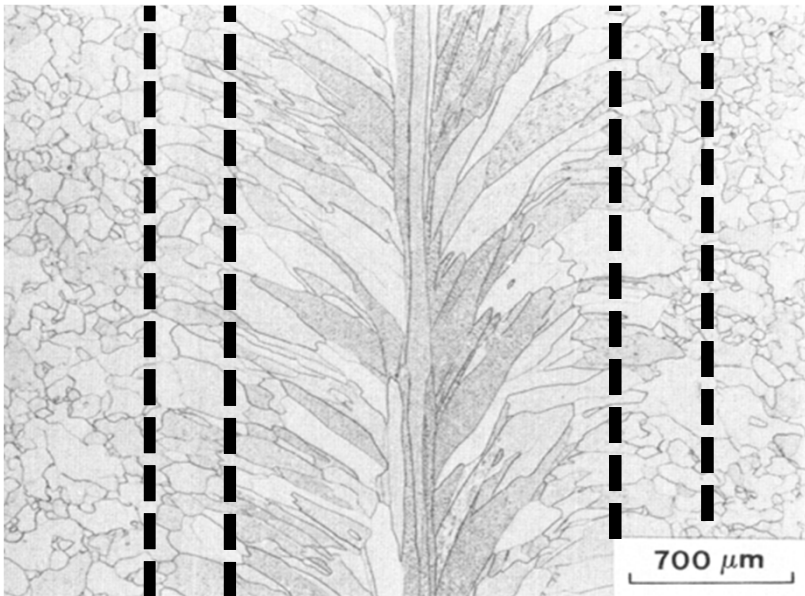
Grains grow epitaxially,
perpendicular to iso-temperature
lines



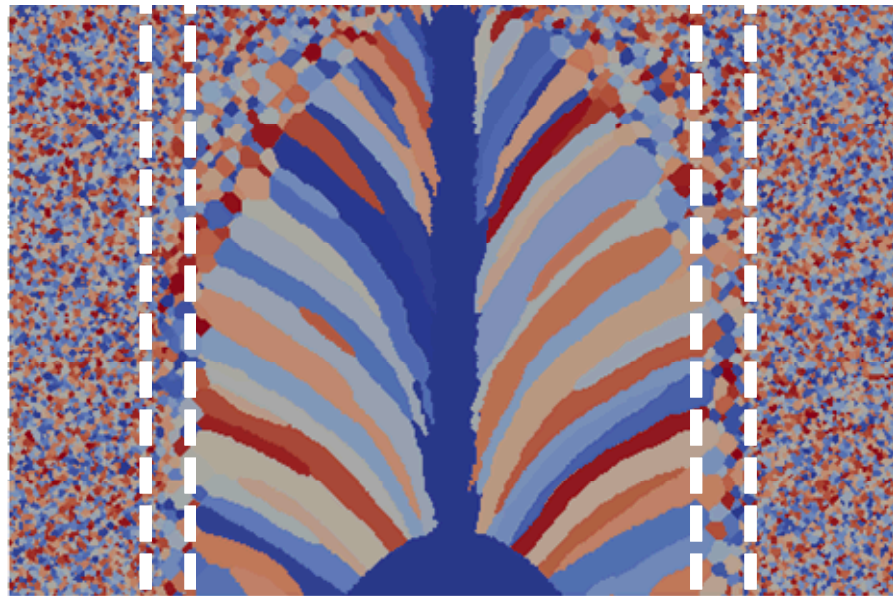
Experiment/Simulation Comparison

bead width = 2.5 mm
weld speed = 760 mm/min
weld grain size = 184 μm

spot size = 2.5 mm
heat source travel rate = 760 mm/min
weld grain size = 190 μm



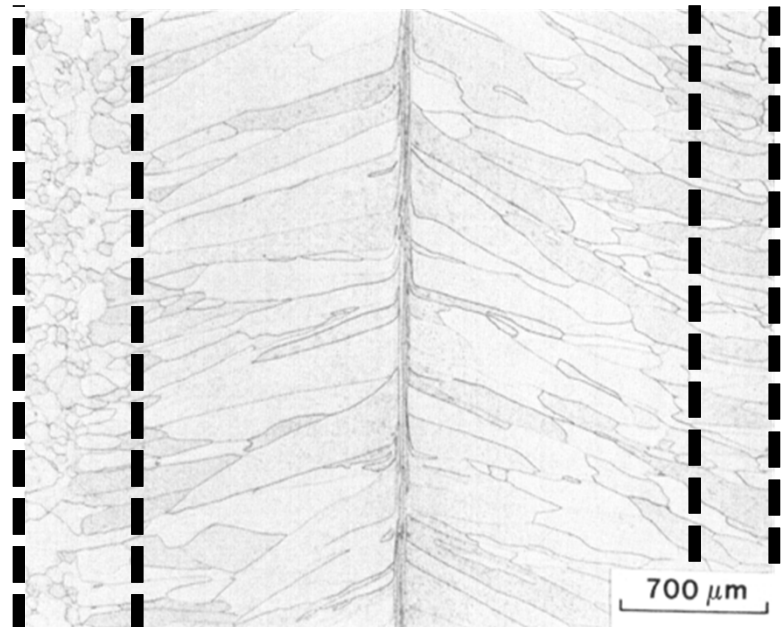
C. Liu & S. David, *Met Trans A*, vol. 13 A, (1982)



← Bead Width = 2500 μm →
 ← HAZ = 3125 μm →

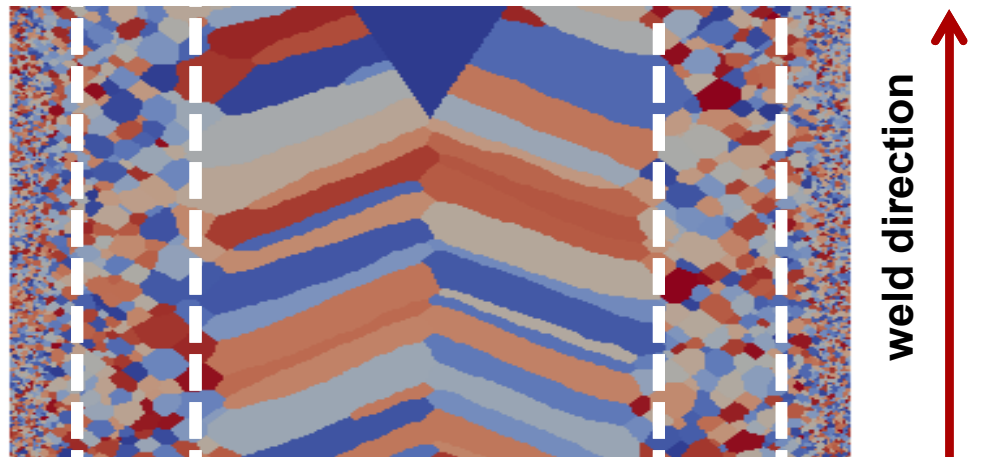
Experiment/Simulation Comparison

bead width = 3.7 mm
weld speed = 760 mm/min
weld grain size = 142 μm



C. Liu & S. David, *Met Trans A*. vol. 13 A, (1982)

spot size = 3.7 mm
heat source travel rate = 760 mm/min
weld grain size = 179 μm

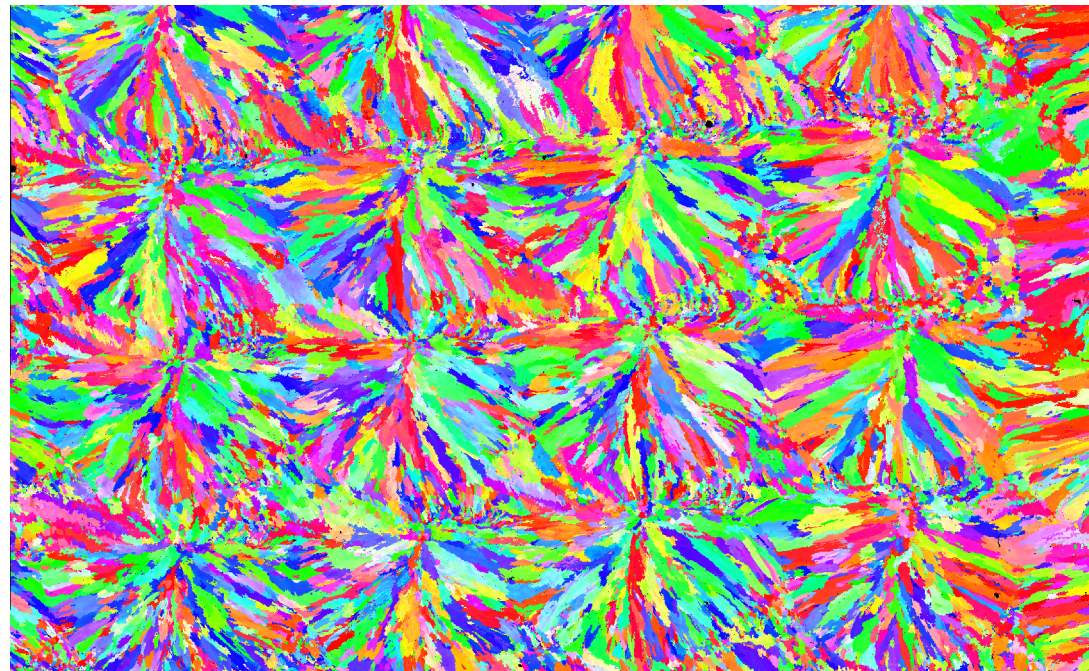
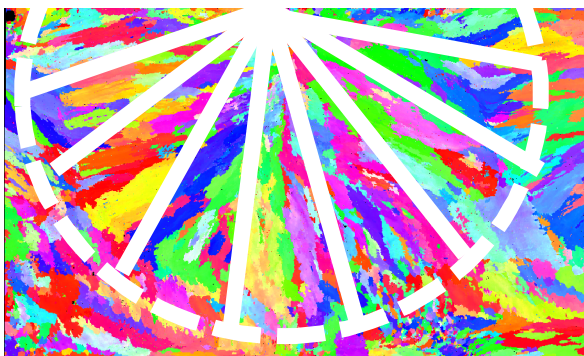


← Bead width
 = 3700 μm →
 ← HAZ = 4374 μm →

Summary

- Developed and demonstrated a user-routine for SPPARKS which predicts experimental grain morphologies in the vicinity of a moving heat source
- SPPARKS simulation routine accepts the following as user inputs:
 - Initial grain size
 - Welding spot size
 - Welding spot shape
 - Beam travel speed
- SPPARKS simulation routine provides meso-scale grain predictions for welds in both 2 and 3-dimensions

Application to Additive



J. Michael (1800)
Montage EBSD Map
Laser Engineering Net Shape

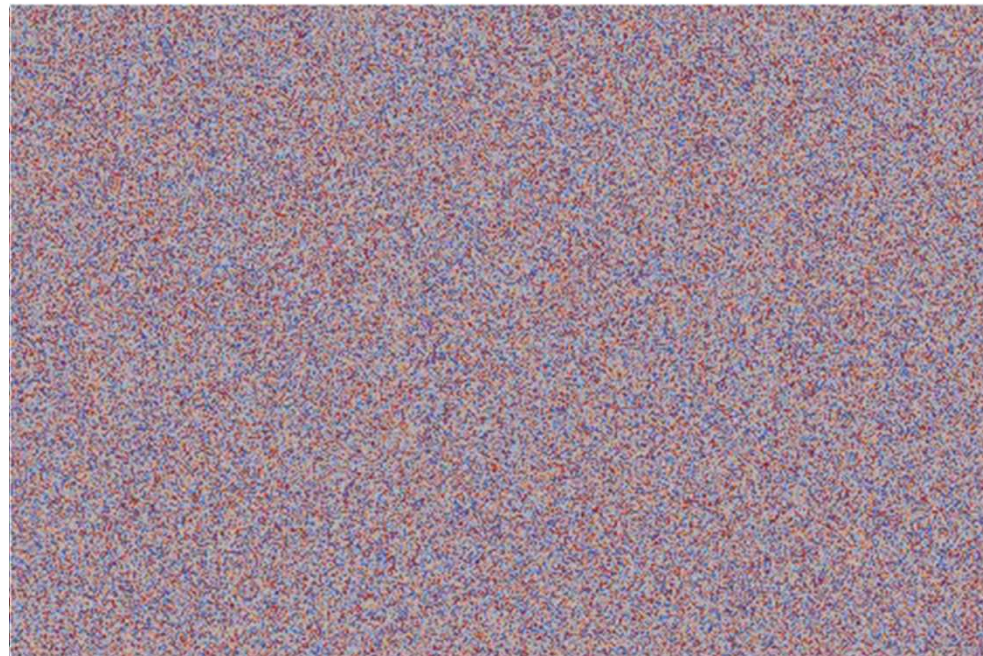
- *Crosshatched*
 - *2 KW*

Simulate Solidification and Grain Growth with Correct Kinetics.

Initial grain size = $25 \mu\text{m}$

X-dim = $4690 \mu\text{m}$

Velocity = 76 cm/min



← Bead width = $2500 \mu\text{m}$ →
← HAZ = $3125 \mu\text{m}$ →

Algorithm Components

KINETIC MONTE CARLO



CELLULAR AUTOMATA



Stochastic, probability driven evolution

C.C. Battaile, The Kinetic Monte Carlo Method: Foundation, Implementation, and Application, Computer Methods in Applied Mechanics and Engineering, 197 (2008) 3386-3398.

H. Barreto, F.M. Howland, Introductory Econometrics: Using Monte Carlo Simulation with Microsoft Excel, Cambridge University Press, New York, 2006.

H.T. MacGillivray, R.J. Dodd, Monte-Carlo Simulations of Galaxy Systems II: Static Properties for Galaxies in Rich Clusters, *Astrophysics and Space Science*, 83 (1982) 127-142.

H.T. MacGillivray, R.J. Dodd, B.V. McNally, J.F. Lightfoot, H.G. Corwin Jr, S.R. Heathcote, Monte-Carlo Simulations of Galaxy Systems I: The Local Supercluster, *Astrophysics and Space Science*, 81 (1982) 231-250.

D.K. Umberger, J.D. Farmer, I.I. Satija, A Universal Strange Attractor Underlying the Quasiperiodic Transition to Chaos, *Physics Letters A*, 114 (1986) 341-345.

P. Landau, K. Binder, A Guide to Monte Carlo Simulations in Statistical Physics, 2nd ed., Cambridge University Press, Cambridge, 2005.

A.D. Rollett, P. Manohar, The Monte Carlo Method, in: D. Raabe, F. Roters, F. Barlat, C. Long-Qing (Eds.) *Continuum Scale Simulation of Engineering Materials*, Wiley-VCH, Strauss GmbH, Morlenbach, 2004, pp. 77-114.

Deterministic, rule-based evolution

[37] K. Janssens, Cellular Automata, in: K.G.F. Janssens, D. Raabe, E. Kozeschnik, M.A. Miodownik, B. Nestler (Eds.) *Computational Materials Engineering: An Introduction to Microstructure Evolution*, Elsevier, Inc., Burlington, MA, 2007, pp. 109-150.

[38] D. Raabe, Cellular, Lattice Gas, and Boltzmann Automata, in: D. Raabe, F. Roters, F. Barlat, L.-Q. Chen (Eds.) *Continuum Scale Simulation of Engineering Materials: Fundamentals-Microstructures-Process Applications*, Wiley-VCH, Strauss GmbH, 2004, pp. 57-76.

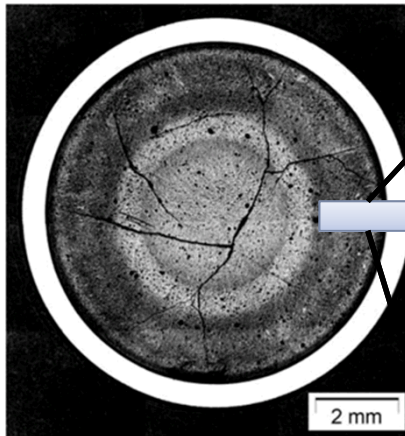
[39] D. Raabe, Yield Surface Simulation for Partially Recrystallized Aluminum Polycrystals on the Basis of Spatially Discrete Data, *Computational Materials Science*, 19 (2000) 13-26.

[40] D. Raabe, Mesoscale Simulation of Recrystallization Textures and Microstructures, *Advanced Engineering Materials*, 3 (2001) 745-752.

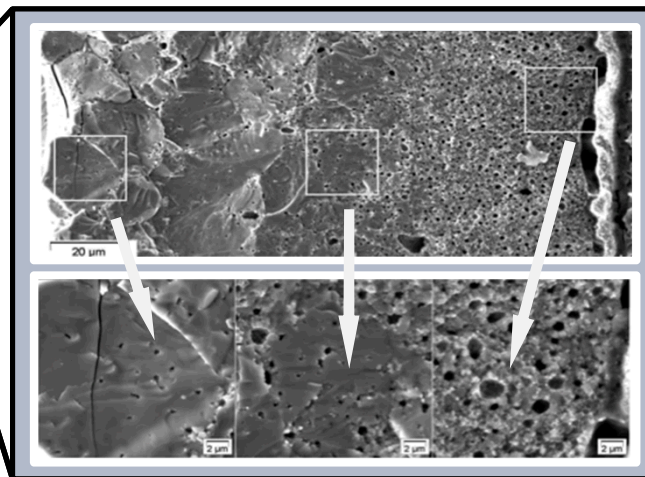
Background II

- We are interested in recrystallization for 2 primary reasons
 - Common occurrence in engineered metals undergoing large-scale deformation (e.g. rolling)
 - Proposed as the evolutionary process responsible for the 'rim effect' in nuclear fuels

Nuclear Fuel Pellet
www.nrc.gov



Irradiated Fuel Cross-Section
Noirot, et. al *NE&T*, vol. 41 2009

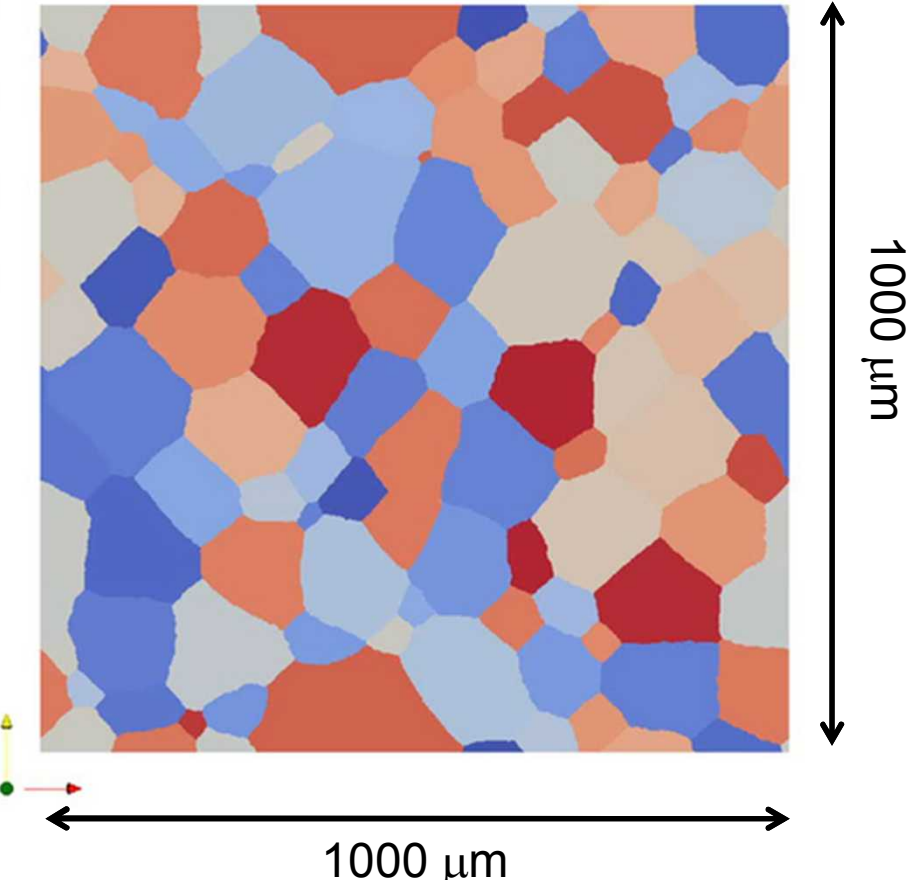
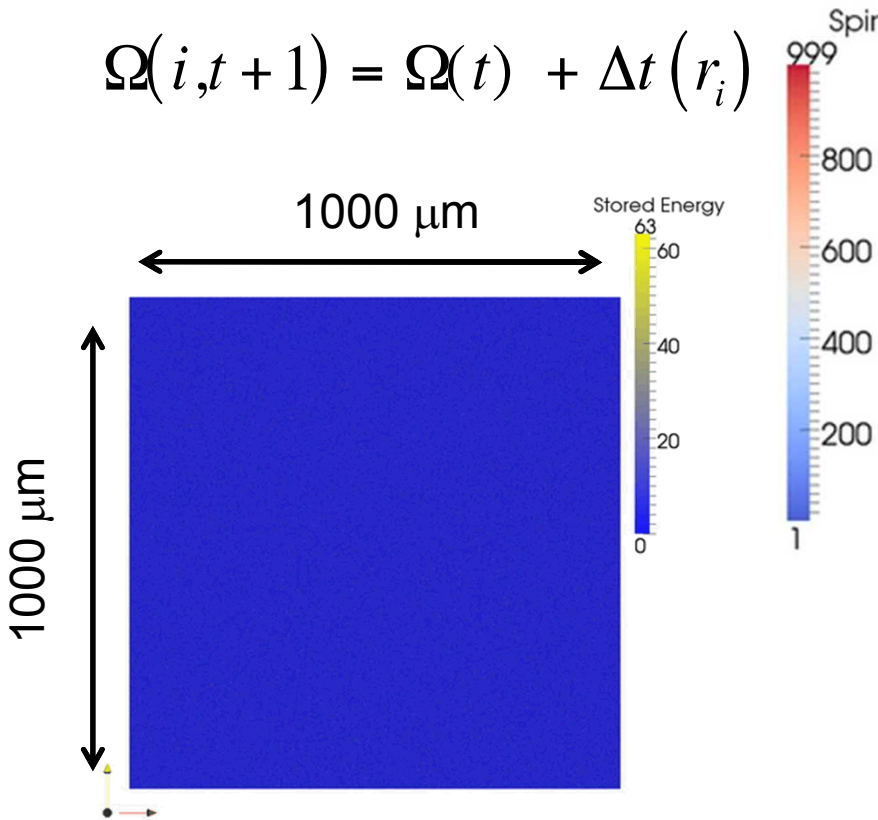


RESULT

Tremendous Variation In Microstructure

1. Grain size
2. Porosity
3. Percolation
3. Composition
4. Hardness

Background III

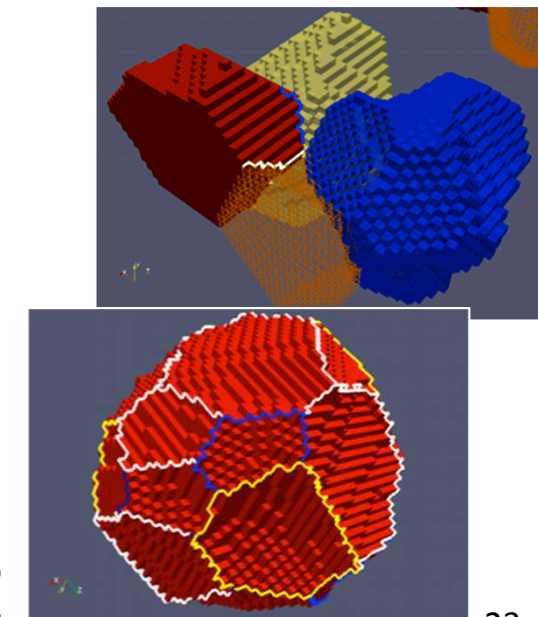
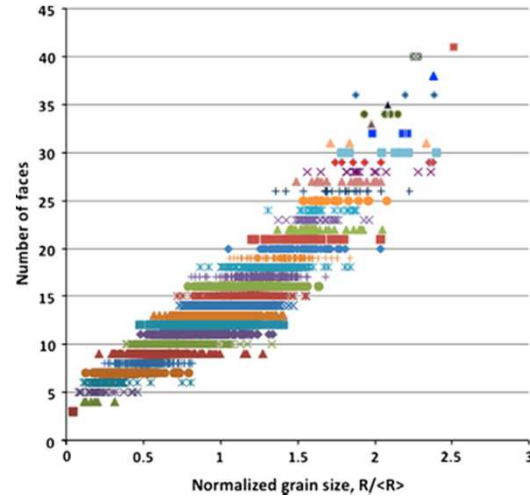
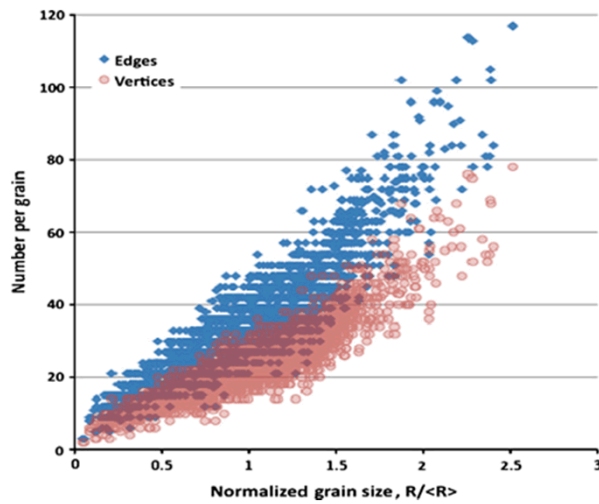


8 MCS / frame
 1000 spins
 1000 x 1000 x 1
 Initial Grain Size $\langle R \rangle = 100$
 Average $\langle R \rangle$ During Recrystallization = 5

User Defined parameters: (g) threshold, (η) nucleation rate, (M) boundary mobility, (r) recrystallization rate

Background IV

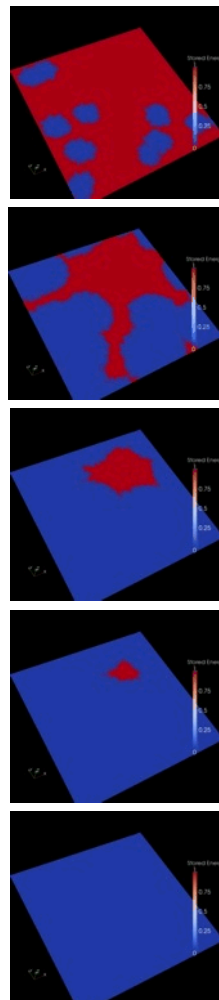
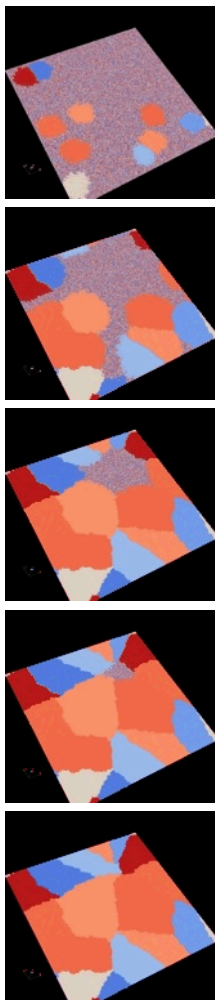
- Topological changes during grain growth are thought to control microstructural evolution
- Here we apply a recently developed automated method[❖] to characterize topology in digital microstructures, to simulations of 2D static recrystallization



[❖] Z. Sun, V. Tikare, B. R. Patterson and A. P. Sprague: *Comp. Mat. Sci.*, 2012, vol. 55 pp. 329-36.

C.A. for Recrystallization

Binary Energy Case [$e = 1$ or 0]
2Dimensional, Site Saturated



spins

stored energy

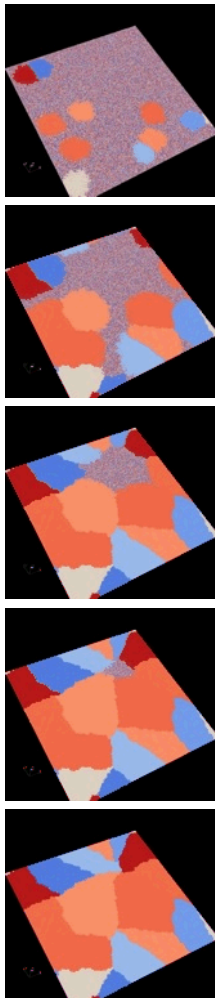
$$\text{if } \Omega_i < \Omega_j^{\text{initial}} \left\{ \begin{array}{l} \Omega_j = \Omega_i \\ \text{spin}_j = \text{spin}_i \end{array} \right.$$

Although the CA approach is entirely stored energy dependent, changes of spin accompany all recrystallization events. Should a neighboring grain possess a higher energy, under recrystallization, that grain will inherit both the lower stored energy and spin of the adjacent grain

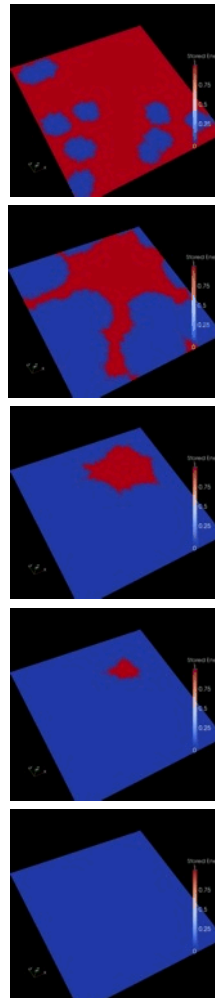
$$\Delta E_{i,RC} = \Omega_i^{\text{final}} - \Omega_i^{\text{initial}} \quad P = \begin{cases} 0 & \text{if } \Delta E > 0 \\ \frac{|\Delta E_{i,RC}|}{\Omega^{\text{MAX}}} & \text{if } \Delta E \leq 0 \end{cases}$$

C.A. for Recrystallization

Binary Energy Case [$e = 1$ or 0]
2Dimensional, Site Saturated



spins



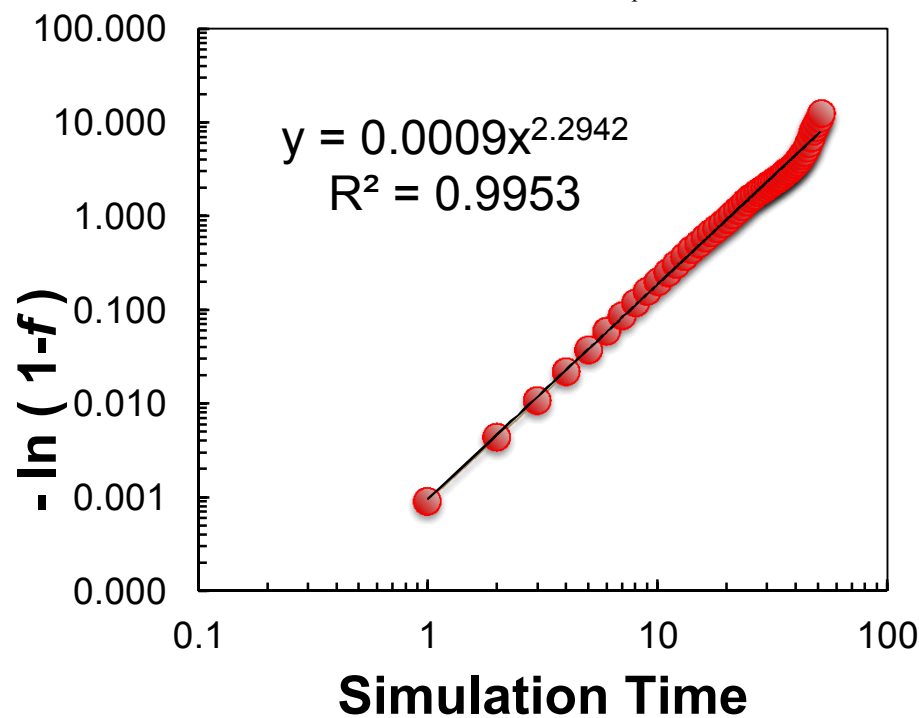
stored energy

Spins = 100

Total Sites = 250 000

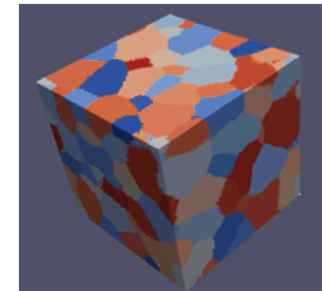
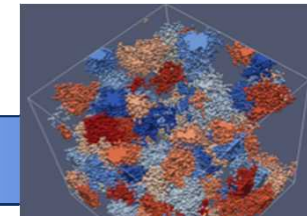
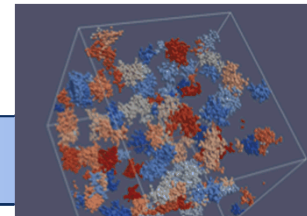
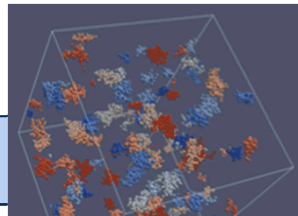
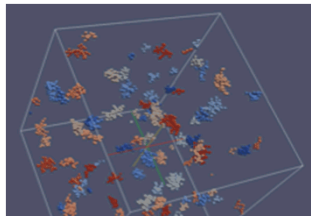
Total N_{accepted} = 247 418

$$(1-f) = \frac{(\text{Total } N_{\text{accepted}} - N_{\text{accepted}})}{\text{Total } N_{\text{accepted}}}$$

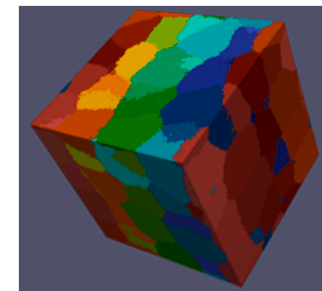
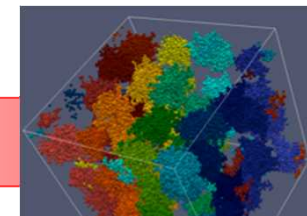
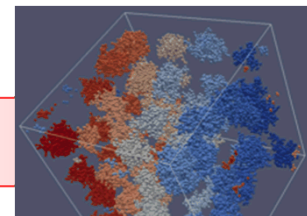
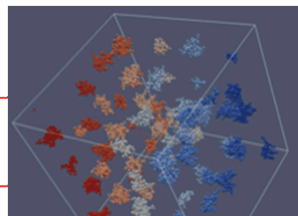
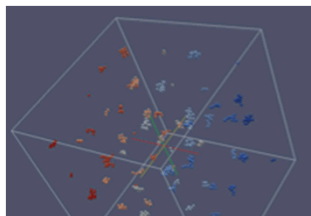


Nuclei Instantiation

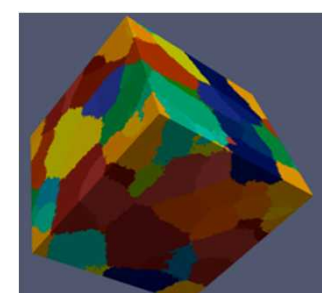
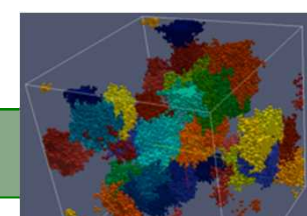
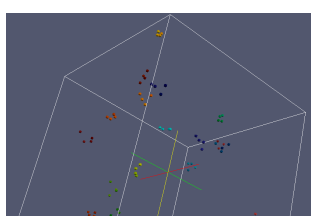
Nuclei are “seeded” into the simulation domain in one of three ways;
1) random, 2) ordered, or 3) clustered



RANDOM

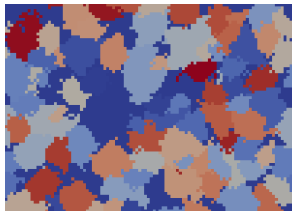


ORDERED

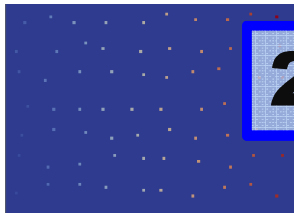


CLUSTERED

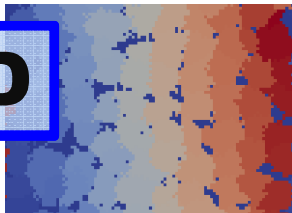
2D & 3D Domains



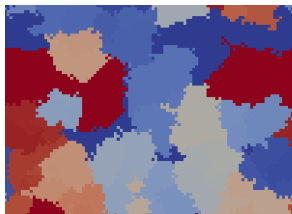
RANDOM



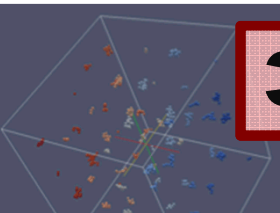
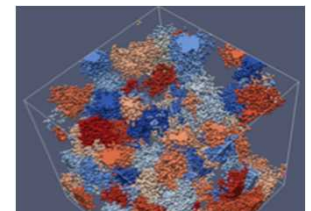
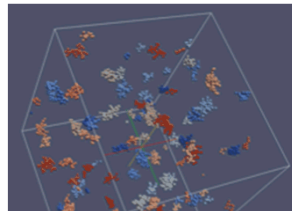
2D



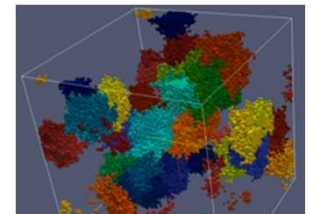
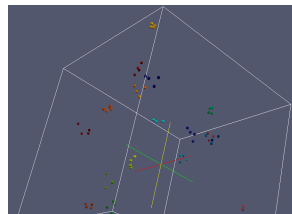
ORDERED



CLUSTERED



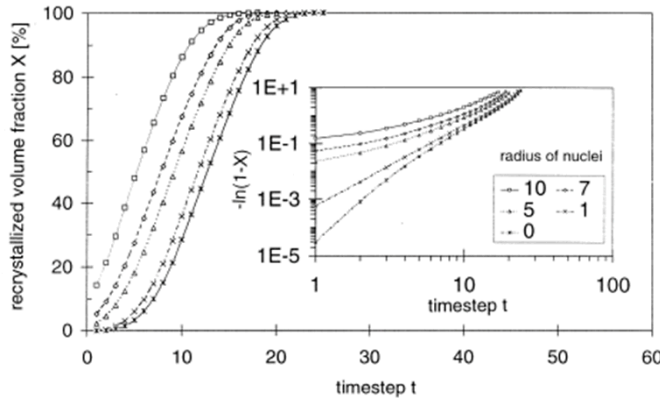
3D



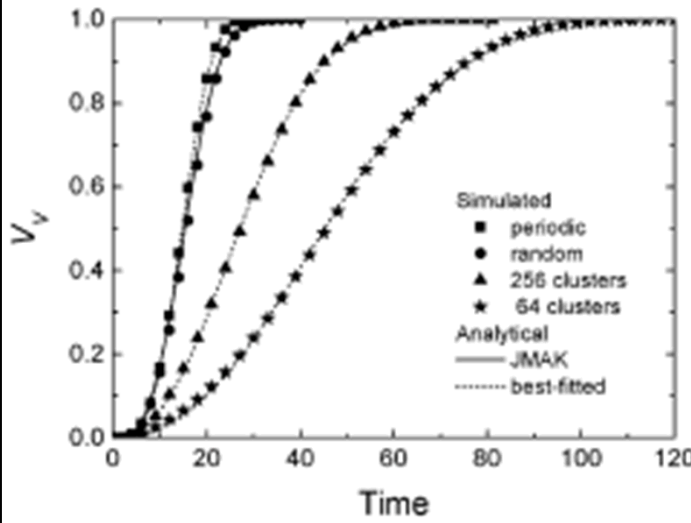
500 x 500 x 1
Instantiated Nuclei = 1000 = 0.4%
Site saturated Static ReX

100 x 100 x 100
Instantiated Nuclei = 1000 = 0.1%
Site Saturated Static ReX

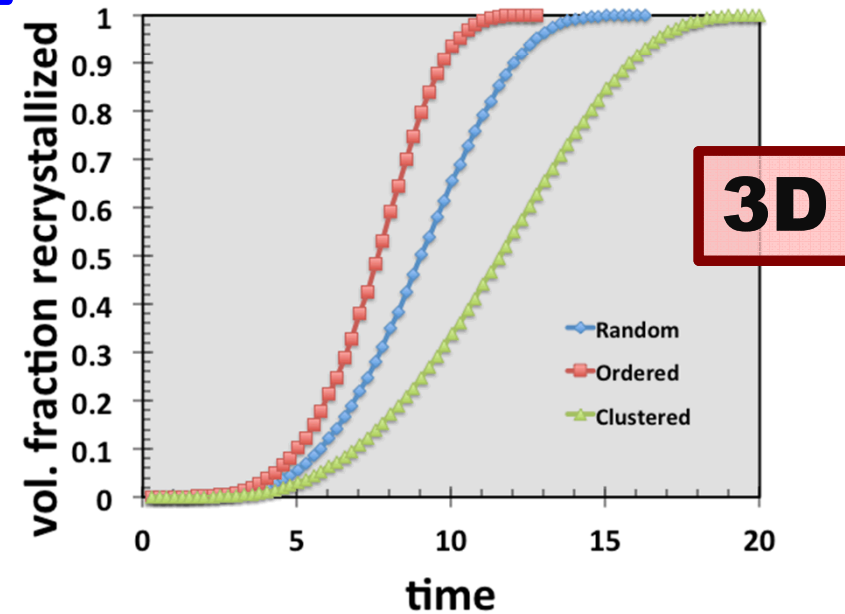
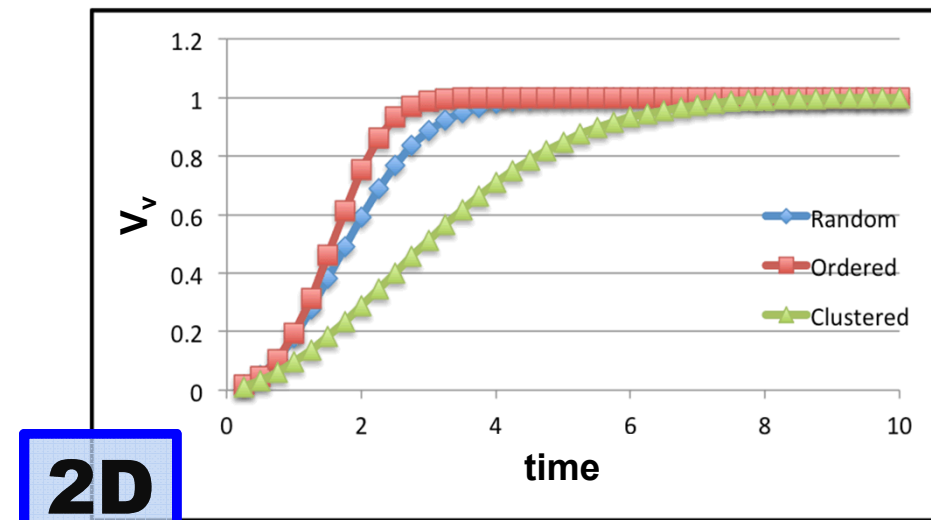
Volume Fraction



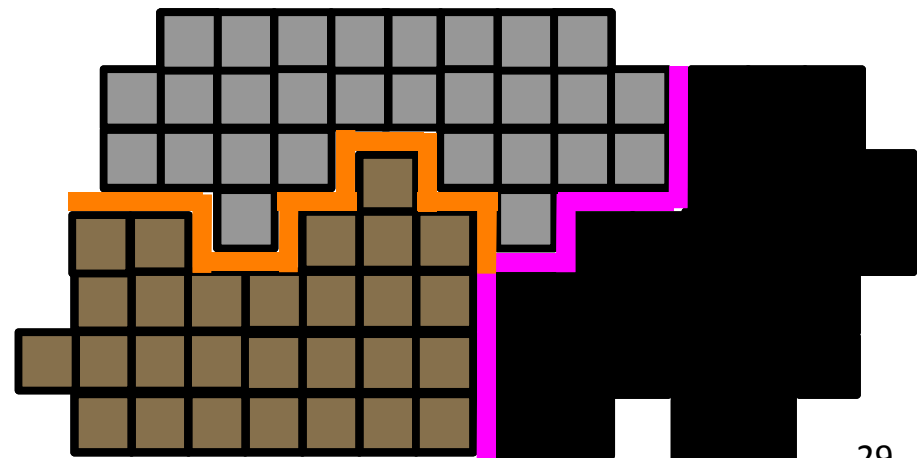
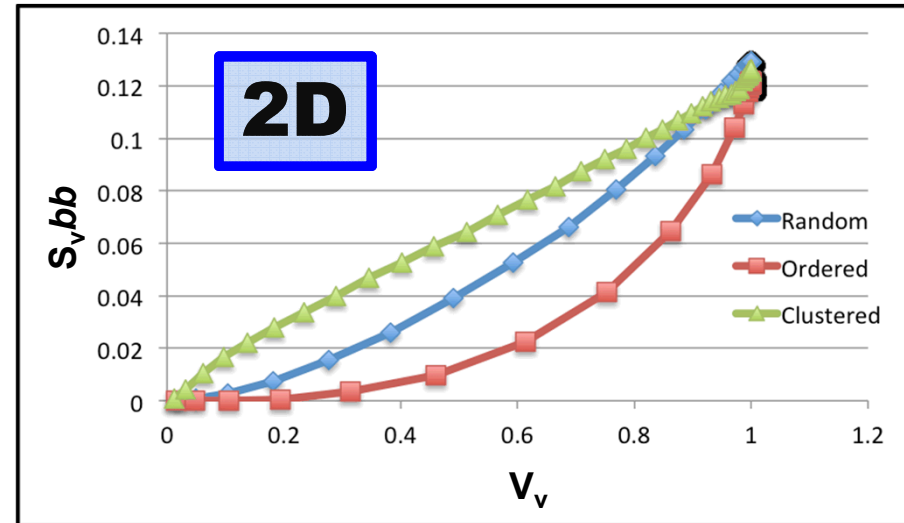
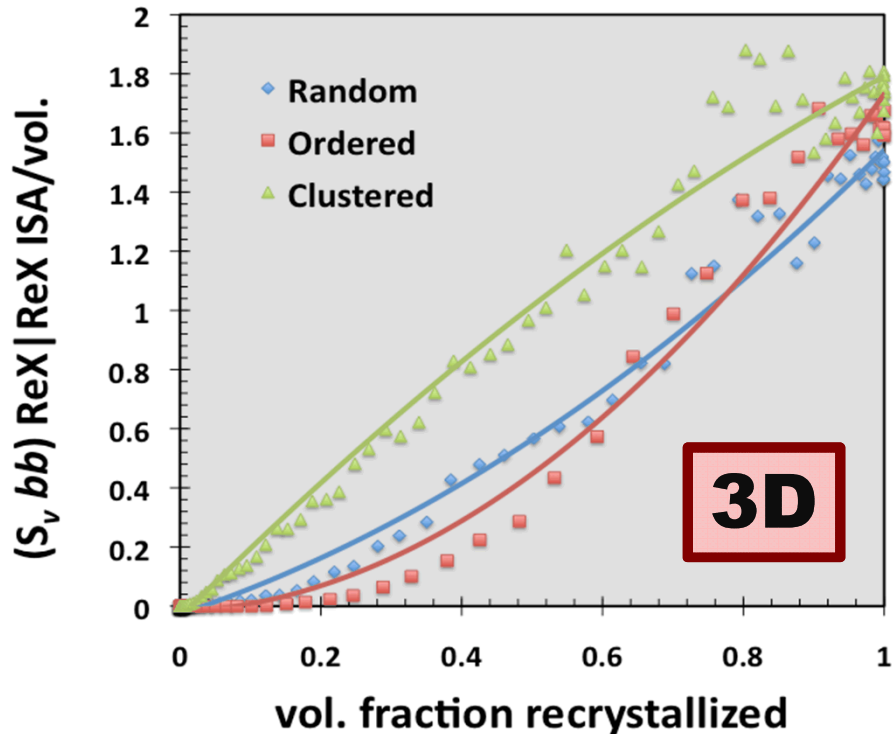
Marx et al: *Acta Mat.*, 1999, vol. 47
pp. 1219-1230.



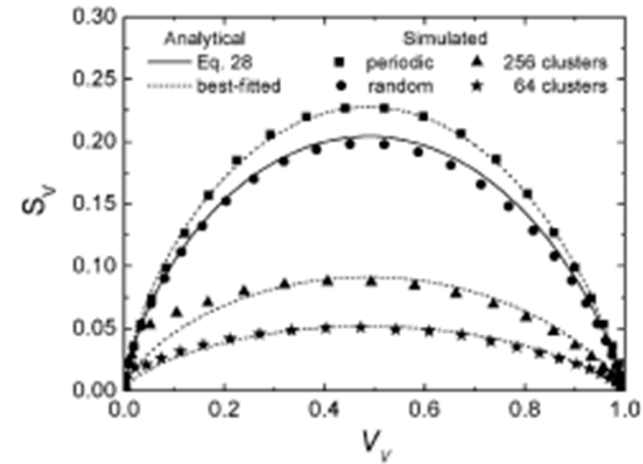
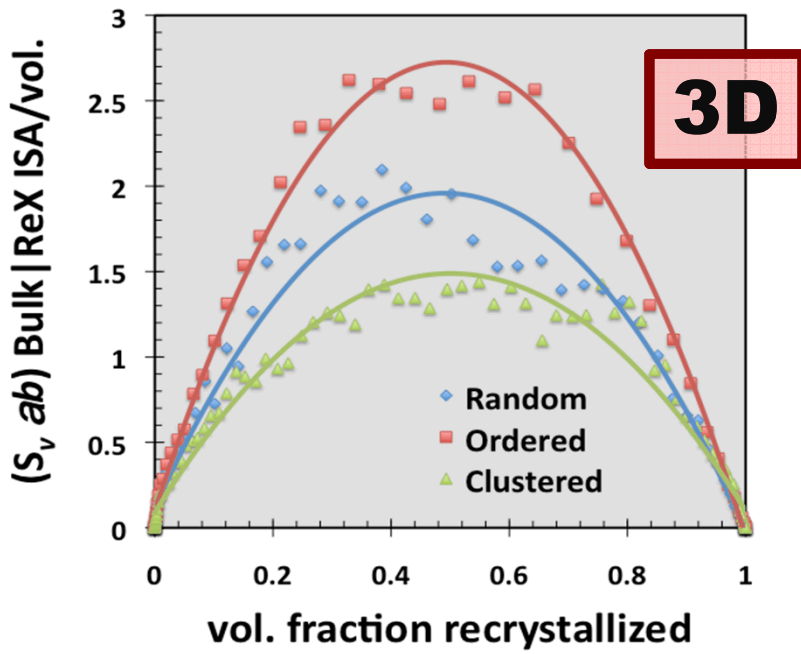
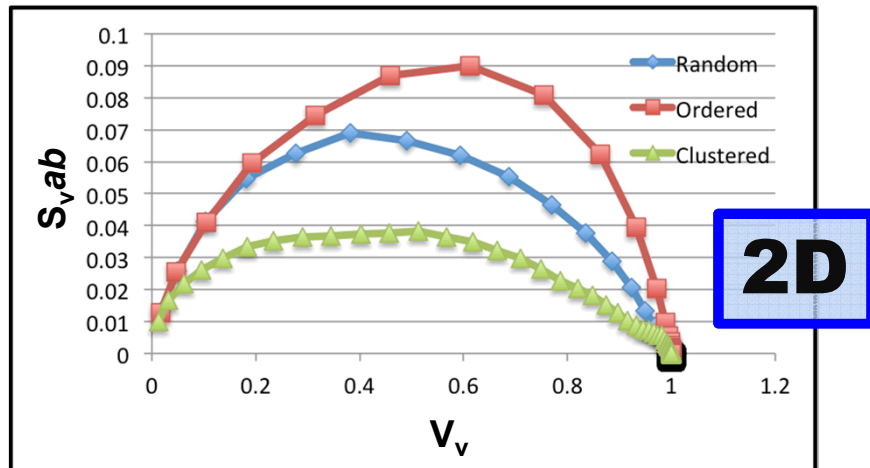
P. R. Rios, L. O. Pereira, F. F. Oliveira, W. L. S. Assis and J. A. Castro: *Acta Mat.*, 2007, vol. 55
pp. 4339-48.



Interfacial Surface Area I

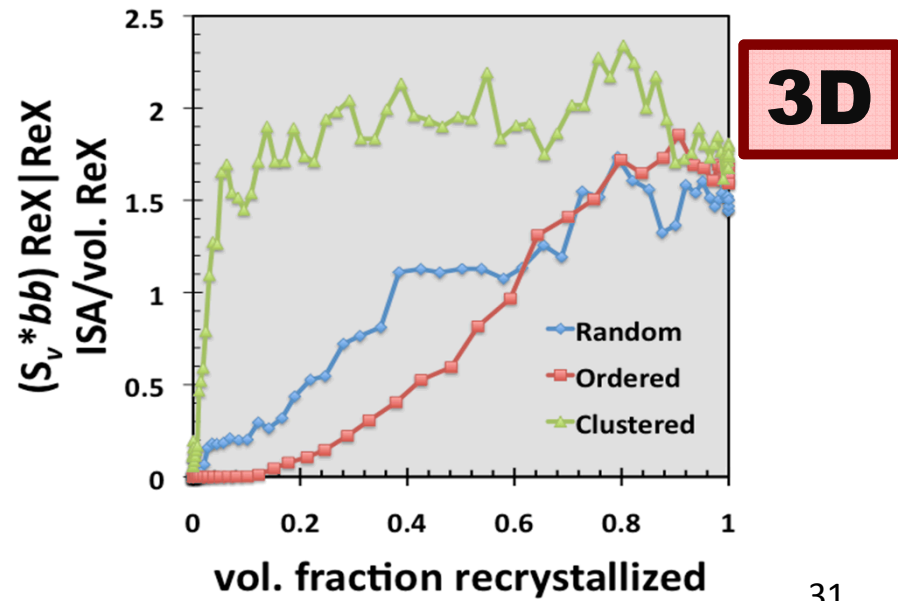
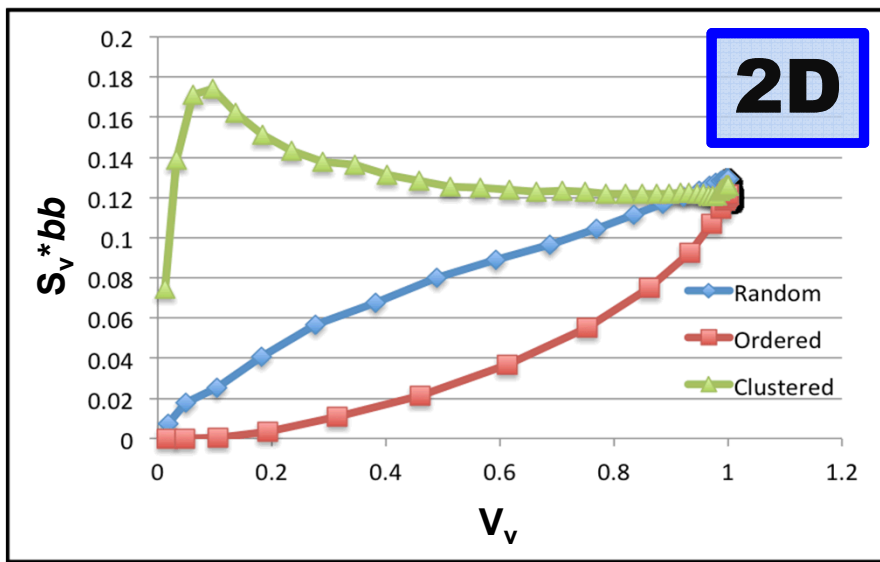
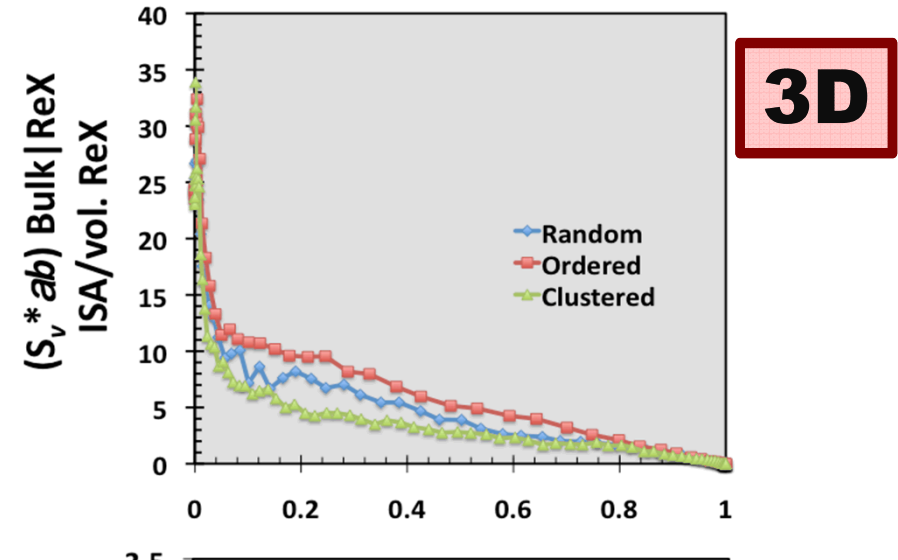
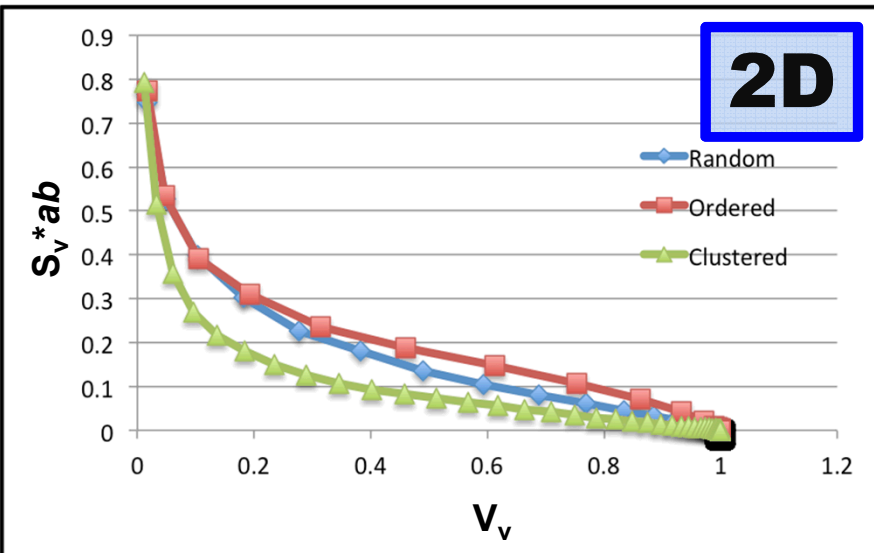


Interfacial Surface Area II

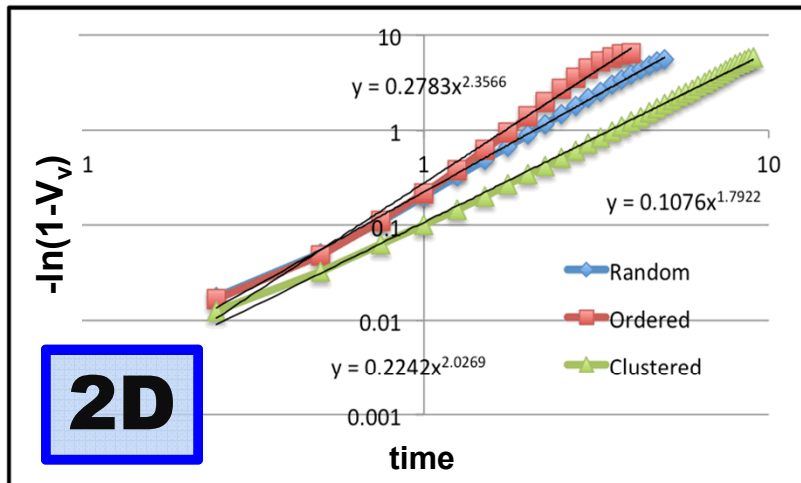


P. R. Rios, L. O. Pereira, F. F. Oliveira, W. L. S. Assis and J. A. Castro: *Acta Mat.*, 2007, vol. 55 pp. 4339-48.

Interfacial Surface Area III



KJMA Exponent



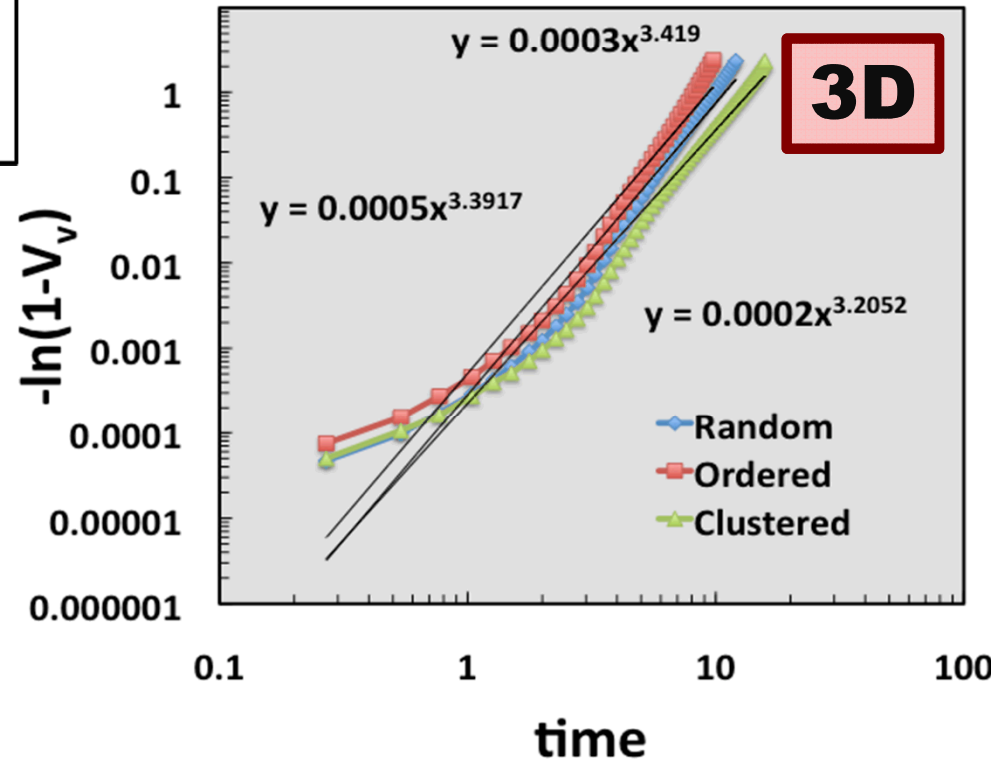
For site saturated nuclei

1D growth : $n \sim 1$

2D growth : $n \sim 2$

3D growth : $n \sim 3$

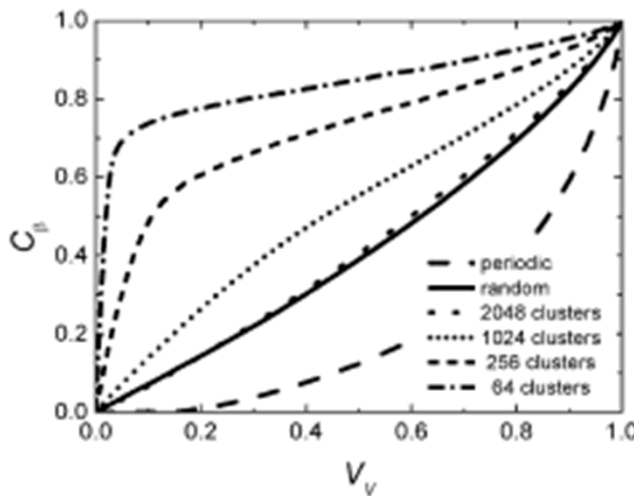
$$\log(-\ln(1 - V_v)) = n \log(t)$$



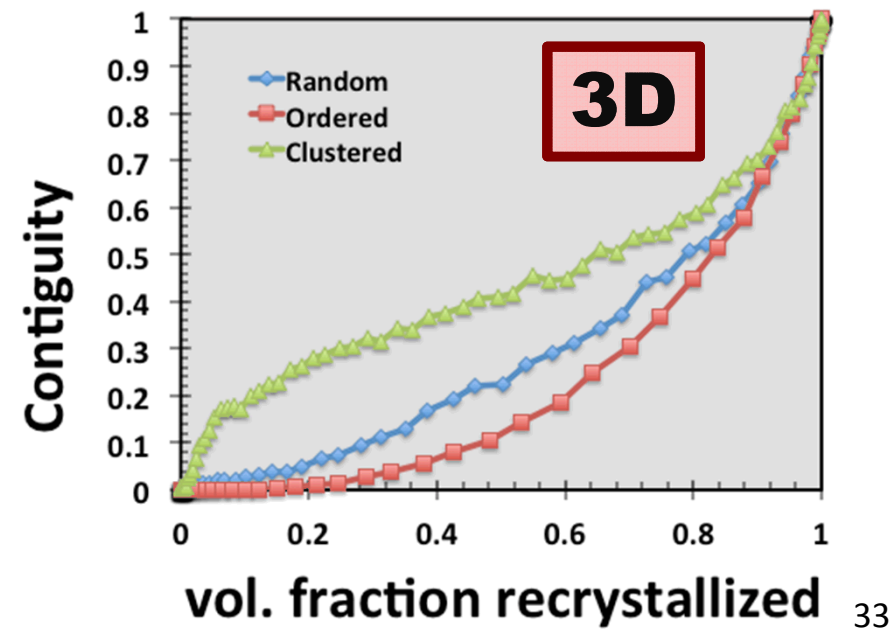
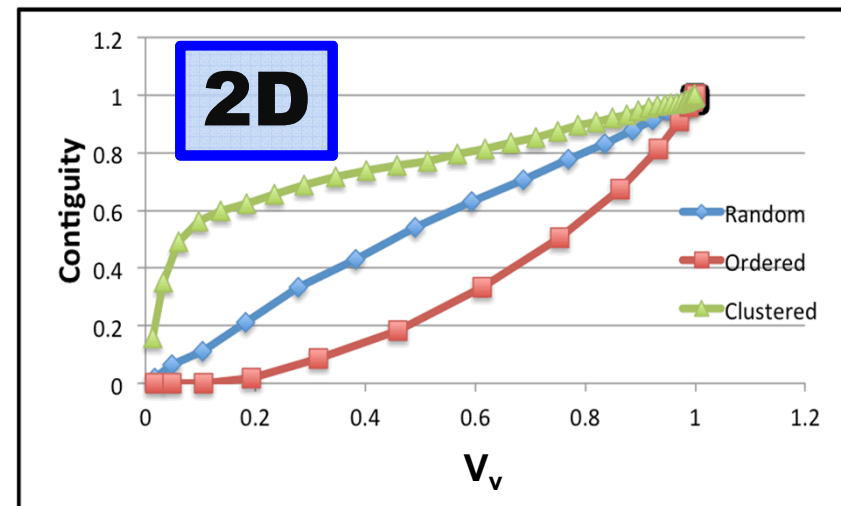
Contiguity

$$C_{\alpha\alpha} = \frac{2(S_v)_{\alpha\alpha}}{2(S_v)_{\alpha\alpha} + (S_v)_{\alpha\beta}}$$

R. Vandermeer: *Acta Mat.*, 2005, vol. 53 pp. 1449-1457.

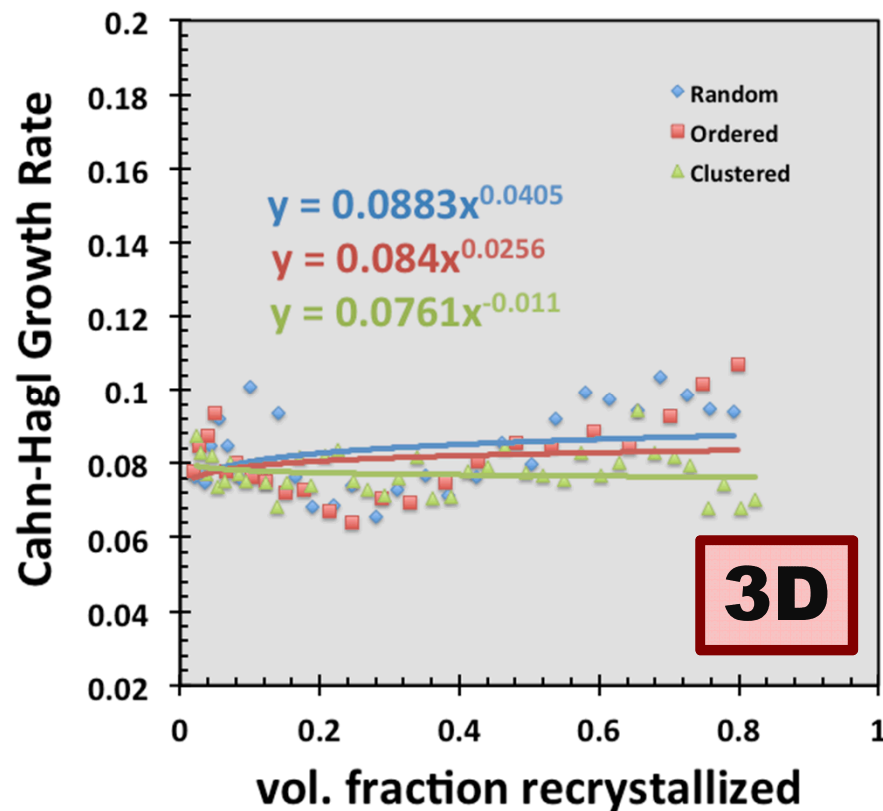
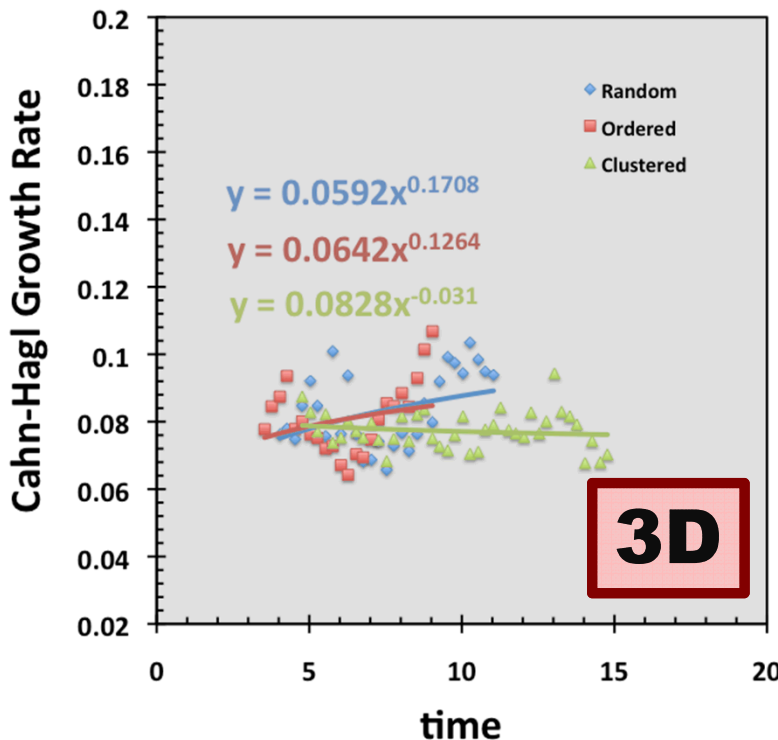


P. R. Rios, L. O. Pereira, F. F. Oliveira, W. L. S. Assis and J. A. Castro: *Acta Mat.*, 2007, vol. 55 pp. 4339-48.

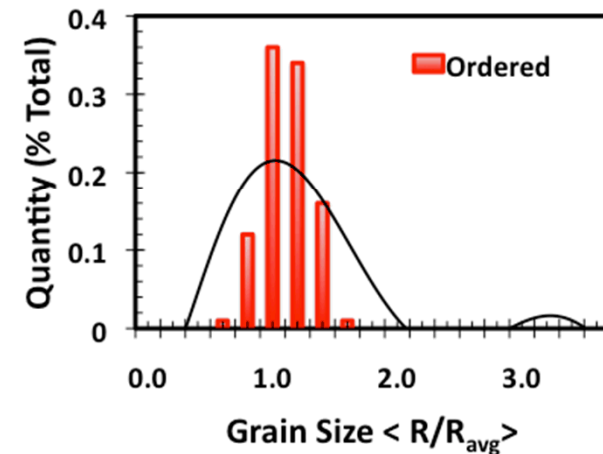
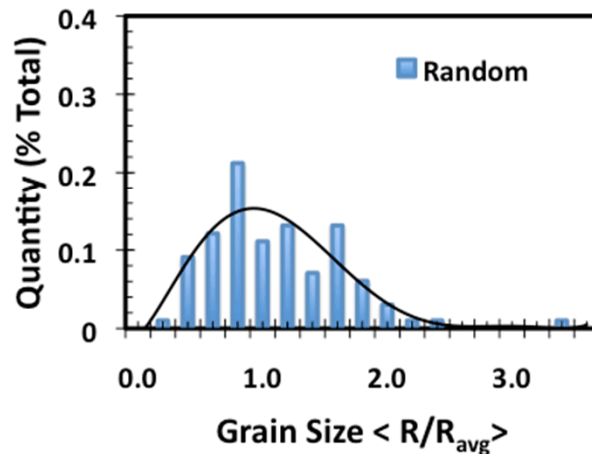
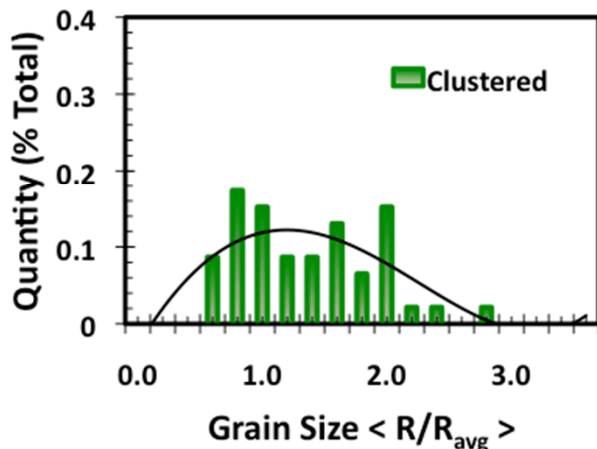


Cahn-Hagel Growth Rate

$$G_{Cahn-Hagel} = \left[\frac{1}{S_V} \right] * \left[\frac{dV}{dt} \right]$$



Grain Size Distributions



Coefficient of variation (CV)

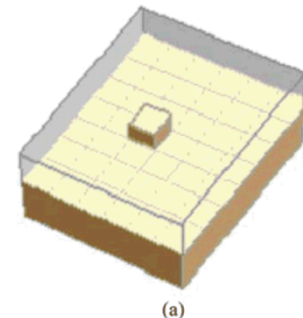
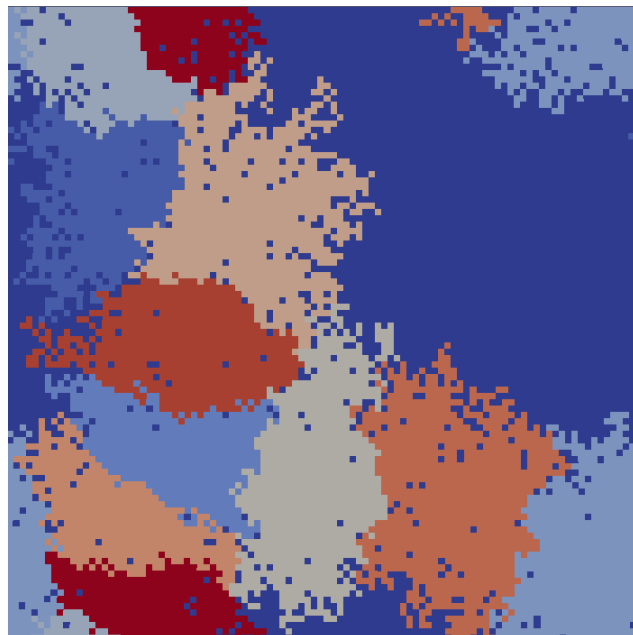
$$CV = \frac{\sigma}{\mu} = \frac{st. \text{ deviation}}{mean}$$

Provides extent of variability in relation to the mean of a population

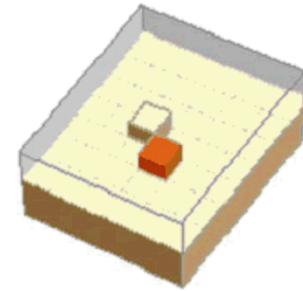
	Clustered		Random		Ordered	
	R_{avg}	C.V.	R_{avg}	C.V.	R_{avg}	C.V.
0.10 V_v	401	0.46	244	0.32	260	0.26
0.50 V_v	1935	0.56	1273	0.34	1234	0.14
1.00 V_v	3906	0.71	2525	0.55	2499	0.18

Future Work

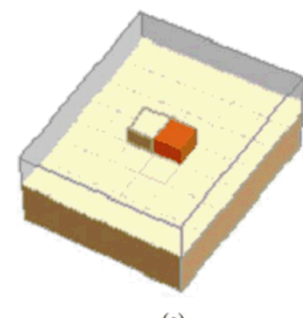
- Initial work shows enhanced surface roughness when employing three dimensions. This artifact has been denoted as “the model-lattice effect” by other investigators.



(a)



(b)



(c)

*O. M. Ivasishin, et al., Mater. Sci. Eng. A,
2006, vol. 433 pp. 216-232.*

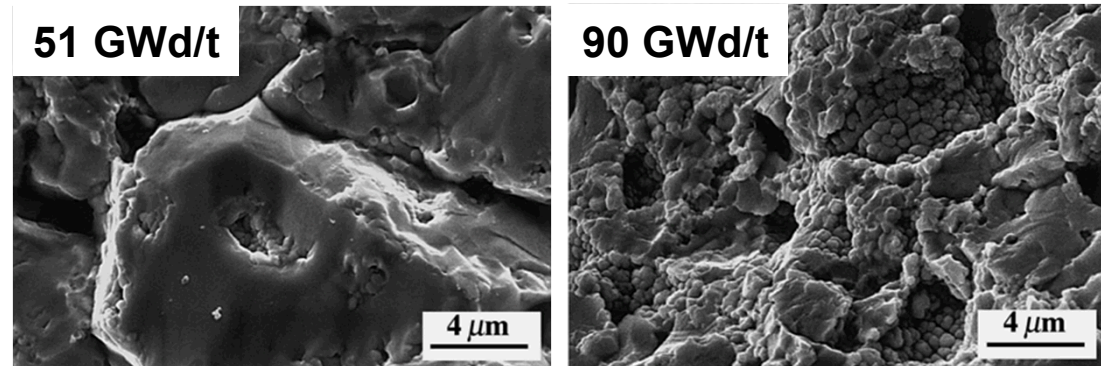
Summary

- The kMC-C.A. hybrid model viably mimics static recrystallization behavior in both 2 and 3 dimensions.
- The hybrid model represents a readily deployable methodology modeling recrystallization in simple systems and tracking microstructural evolution inclusive of;
 - interfacial surface areas,
 - KJMA exponents,
 - contiguity,
 - Cahn-Hagel growth rate
- While 3d simulations exhibit enhanced roughening, tracked features show reasonable agreement with trends previously identified by Rios et al., Marx et al. and Vandermeer

Questions

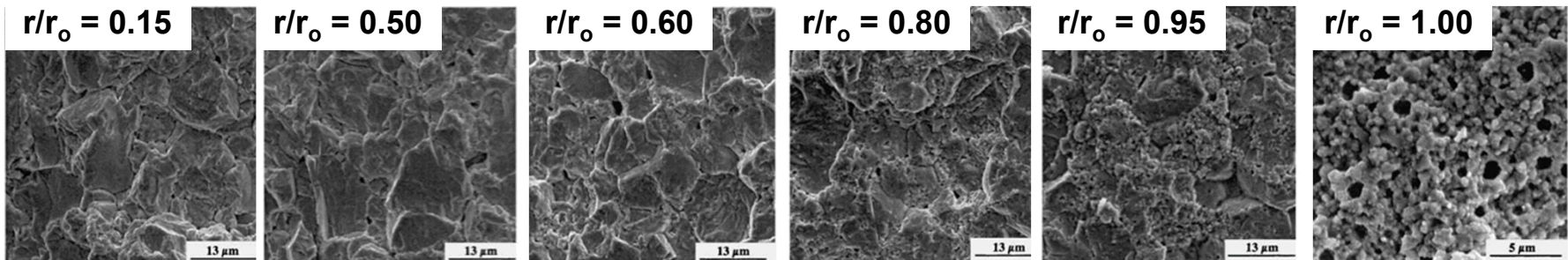
High Burn-Up Structure I

- Rim structure is a function of burn-up
- Low burn-up, original grain structure
- With ^{239}Pu formation, recrystallization occurs where enrichment is most pronounced



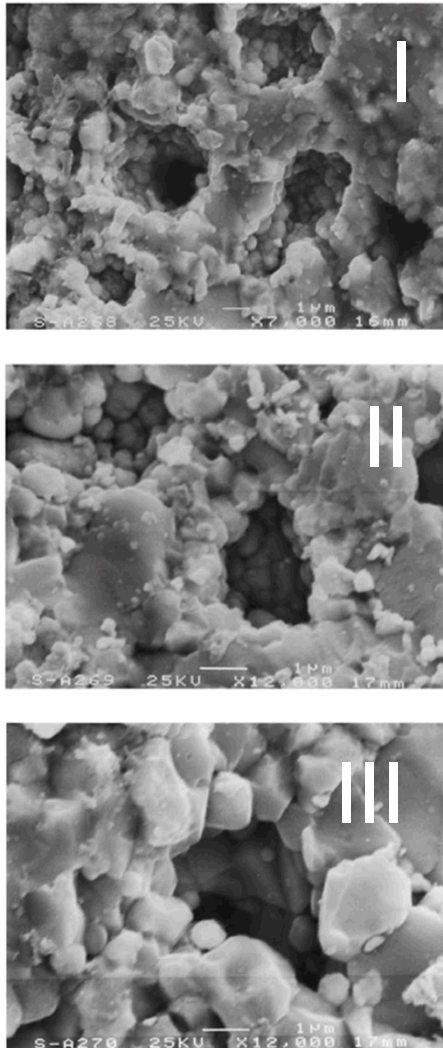
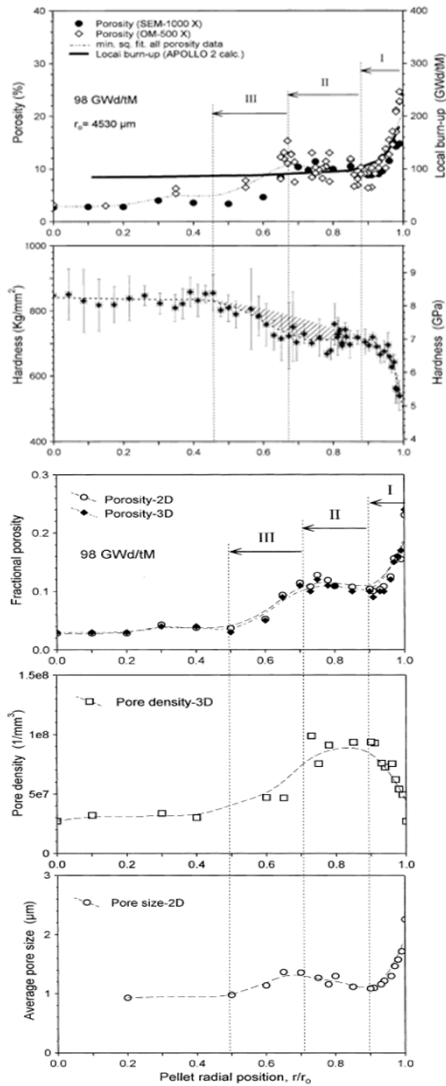
Une, et. al, *JNM* vol. 288, 2001

- Since burn-up correlates with radial position recrystallization is largely absent as r/r_o decreases



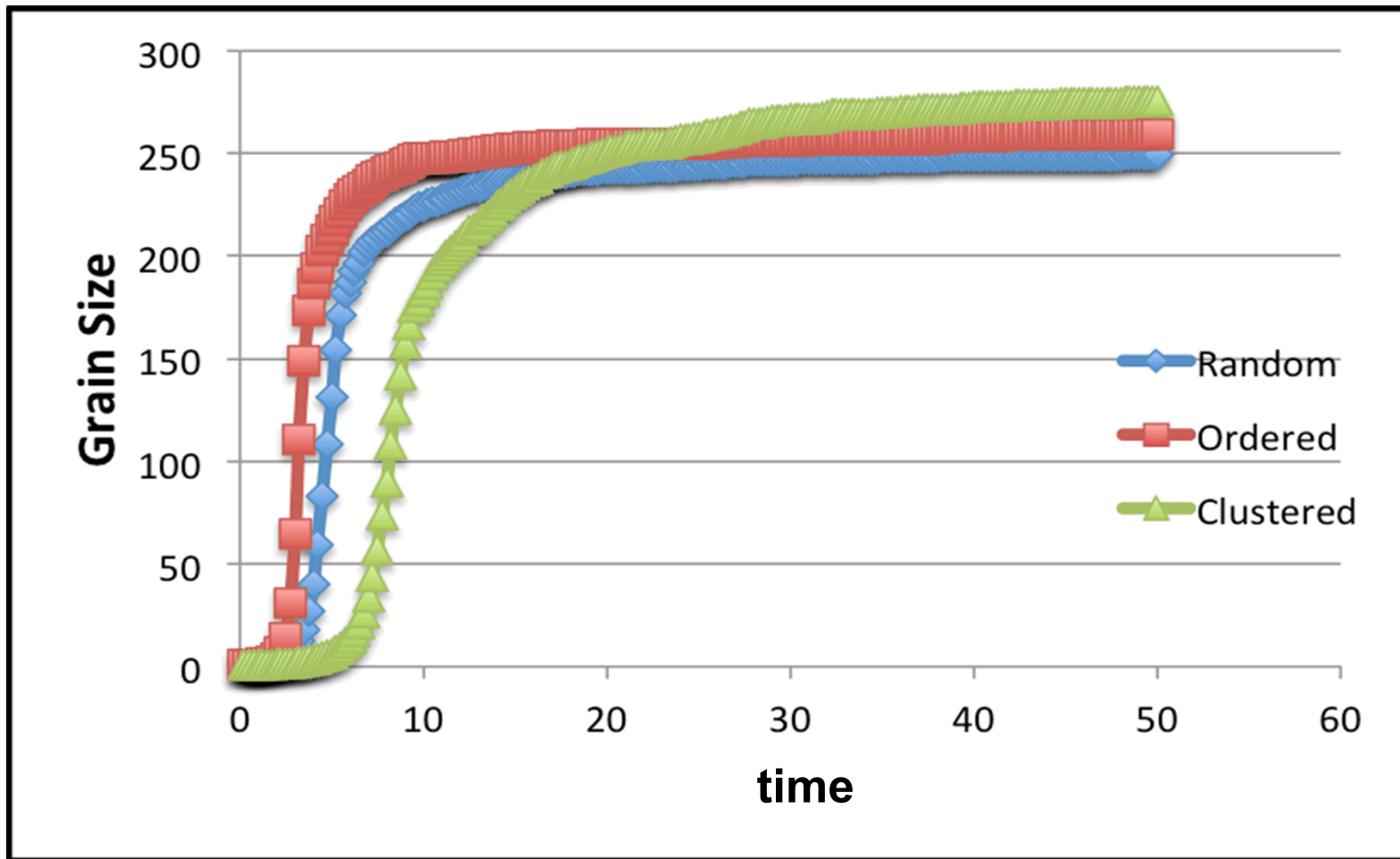
Manzel & Walker, *JNM* vol. 301, 2002

High Burn-Up Structure II



- Understanding the rim effect is important
 - Effects fuel performance (thermal conductivity, fission product distributions, ...)
 - Effects mechanical properties during storage and transportation
 - Modifies the separation processes for fuel recycling.
- Various aspects of the evolutionary process are analogous to metallic systems undergoing dynamic recrystallization.

Grain Size



Cumulative Frequency Distributions

100%

